

Evaluating Tire Pressure Control System to Improve Productivity and Mitigate Pavement Damage

by

Fazal Mabood

A thesis
presented to the University of Waterloo
in fulfillment of the
thesis requirement for the degree of
Masters of Applied Science
in
Civil Engineering

Waterloo, Ontario, Canada, 2008

©Fazal Mabood 2008

AUTHOR'S DECLARATION

I hereby declare that I am the sole author of this thesis. This is a true copy of the thesis, including any required final revisions, as accepted by my examiners.

I understand that my thesis may be made electronically available to the public.

--

Fazal Mabood

ABSTRACT

The introduction of the use of Tire Pressure Control Systems (TPCS) to improve the productivity of the Canadian trucking industry is gaining momentum. The imposition of seasonal load restrictions (SLR) on the thaw-weakened secondary roads interrupts the transportation of raw materials to processing facilities. For the forestry industry in particular, this has very significant impacts on productivity and costs. FPInnovations-Feric Division (Feric) has investigated the potential for TPCS-equipped trucks to travel with full, legal loading during the SLR period without accelerating road wear and tear. The TPCS monitors and adjusts the inflation pressure of the trucks' tires while driving and allows the operator to optimize the inflations for changes in loading, travel speed, or road quality encountered in the trip.

This thesis describes an investigation to determine whether TPCS can be used to mitigate traffic generated damage to secondary roads and also reduce the need to implement load restrictions. The project involves a partnership with the Ontario Ministry of Transportation Ontario (MTO), Forest Engineering Research Institute of Canada (FERIC), Ontario Ministry of Natural Resources (MNR) and the Centre for Pavement and Transportation Technology (CPATT) located at the University of Waterloo.

The thesis will describe the methodology, design, and instrumentation of the two test sites which are located in Dryden, Ontario and Chapleau, Ontario. In addition, repeated Portable Falling Weight Deflectometer (PFWD) testing is being carried out at these sites and the initial results of this examination and associated impacts of the environment and traffic on the road will be presented. This study also involves looking into the reliability of using the portable FWD, offering a lower cost alternative instead of the trailer mounted FWD to monitor pavement strength for the identification the SLR period. The use of innovative sensors and data collection techniques are proving to be very informative and are advancing pavement engineering knowledge. Moreover, the thesis is aimed at exploring the possibilities of achieving the current objectives of the government DOTs such as TPCS potential for addressing the timber industry in crisis, reduced road maintenance budgets, and global warming increasing road damage.

ACKNOWLEDGEMENTS

Firstly, I would express my gratefulness to my supervisor, Professor Dr. Susan Tighe for her support and guidance throughout this research project, and giving me a chance to be one of her team member at the Center of Pavement and Transportation Technology (CPATT). In addition, her encouragement, supervision, and professionalism are greatly appreciated. Without her these two years would not have been as rewarding or pleasurable.

I would also like to thank Sudip Adhkari, Mohammad Allauddin Ahmad, Terry Ridgeway, Vimy Henderson, Jodi Norris, Rabiah Rizvi, and Wendy Huang for their valuable input during field work and thesis writing. Shelley Bacik's cooperation during the procurement of instrumentation is highly appreciated and commendable.

In addition, I would like to acknowledge the contributions of the Ministry of Transportation of Ontario (MTO), and FPInnovation (formerly Forestry Engineering Research Institute of Canada, FERIC). In particular, I would thank Tom Klement for his feedback, and members of the MTO Regional staff, including Ken Mossop, Irys Steblynski, George Bates, Lemieux Maurice, and Louis Haukenness for their assistance in the field. Steve Mercier's, from FPInnovation, help throughout the field work is also unforgettable.

Finally, I would like to extend my appreciation to the University of Waterloo's Faculty and Staff, to all the Transportation graduate students for the great memories, and of course, to my wife, my daughters, and my son who have always given me support and have been very patient when I had to stay away from home for long periods due to the extensive field work involved in this study.

DEDICATION

I would like to dedicate all the effort and achievement involved in putting this writing together to my ever-loving parents who have always been a source of inspiration for me. May they both live a long, happy, healthy, and a prosperous life.

TABLE OF CONTENTS

LIST OF FIGURES-----	viii
LIST OF TABLES-----	X
Chapter One INTRODUCTION-----	1
1.1 RESEARCH OBJECTIVE-----	1
1.2 OVERVIEW-----	3
1.3 STUDY OUTLINE-----	4
1.4 SCOPE OF STUDY-----	5
1.5 FIELD TESTING-----	7
1.6 PORTABLE FALLING WEIGHT DEFLECTOMETER (PFWD) -----	7
1.7 PFWD TESTING PROCEDURE-----	8
1.8 FALLING WEIGHT DEFLECTOMETER (FWD) -----	9
Chapter Two LITERATURE REVIEW-----	10
2.1 EFFECT OF TIRE PRESSURE ON PAVEMENT STRUCTURE-----	10
2.2 MAXIMUM WHEEL LOAD-----	10
2.3 WHEEL LOAD AND TIRE PRESSURE-----	11
2.4 EQUIVALENT SINGLE WHEEL AXLE LOAD (ESWL) -----	14
2.5 TIRE PRESSURES AND PAVEMENT PERFORMANCE-----	15
2.5.1 PAVEMENT THICKNESS-----	16
2.5.2 STIFFNESS OF BASE AND SUBGRADE-----	16
2.5.3 AXLE LOADS-----	17
2.5.4 AXLE CONFIGURATION-----	17
2.6 CENTRAL TIRE INFLATION STUDIES-----	18
2.6.1 The Federal Highway Authority (FHWA) Study-----	18
2.6.2 Tire Type-----	18
2.6.3 Tests Conducted by Department of Agriculture, US Forest Service-----	19
SUMMARY-----	19
Chapter Three IN-SITU PAVEMENT STRENGTH MONITORING AND CORRELATIONS-----	20
3.1 CALIBRATION TEST SITE-----	20
3.2 TEST SECTIONS-----	20
3.3 PFWD TESTING PROCEDURES-----	21
3.4 Testing Period-----	21
3.5 Testing Pattern-----	21
3.6 Data Collection-----	21
3.7 CORRELATION BETWEEN PORTABLE FALLING WEIGHT DEFLECTOMETER (PFWD), FALLING WEIGHT DFLECTOMETER (FWD) AND BENKELMAN BEAM-----	23
3.7.1 FALLING WEIGHT DEFLECTOMETER (FWD) VERSUS PORTABLE FALLING WEIGHT DEFLECTOMETER (PFWD) -----	24
3.7.2 BENKELMAN BEAM TO FWD-----	24
3.7.3 BENKELMAN BEAM TO PFWD-----	25
3.8 LINEAR REGRESSION MODEL BETWEEN FWD AND PFWD-----	26

3.9	STRUCTURAL EVALUATION OF ONTARIO’S LOW VOLUME ROADS (LVR) IN COMPARISON WITH BRITISH COLUMBIA’S ROADS FOR SLR-----	30
3.10	SEASONAL LOAD RESTRICTIONS (SLR) PRACTICE AND DURATION-----	31
	3.10.1 SLR IN Ontario-----	32
	3.10.2 SLR in Canada-----	32
3.11	TEST SITES-----	34
	3.11.1 Highway 601-----	34
	3.11.2 Highway 651-----	40
	SUMMARY-----	45
Chapter Four USE OF INNOVATIVE SENSORS, DATA COLLECTION, AND INTERPRETTATION-----		46
4.1	INSTRUMENTATION-----	46
4.2	THERMISTOR STRINGS-----	46
4.3	RELATIVE HUMIDITY AND AIR TEMPERATURE PROBE -----	48
4.4	WATER CONTENT REFLECTOMETER -----	49
4.5	DATA LOGGER CR-1000-----	51
	4.5.1 STORAGE CAPACITY-----	51
	4.5.2 WIRING PANEL-----	52
	4.5.3 POWER SUPPLIES-----	52
4.6	DATA LOGGER PROGRAM AND DATA ACQUISITION-----	54
4.7	DATA ACQUISITION-----	55
4.8	FREEZE THAW PHENOMENON AND REAL TIME DATA-----	56
4.9	MITIGATION OF ROAD DAMAGE USING TPCS EQUIPPED TRUCKS-----	57
4.10	FREEZING/THAWING INDICES, FROST DEPTH, AND THAW DURATION-----	57
4.11	HISTORICAL SLR DATES IN NORTHERN ONTARIO-----	60
	SUMMARY-----	60
Chapter Five ANALYSING THE EFFECT OF LOWERED TIRE PRESSURE ON PAVEMENT-----		61
5.1	OBJECTIVE-----	61
5.2	CENTRAL TIRE INFLATION (CTI) TRIALS ON HIGHWAY 601 AND 651-----	62
5.3	DEVELOPMENT OF DATA AND METHODS OF ANALYSIS-----	65
	5.3.1 Fatigue Criteria of Model-----	65
	5.3.2 Rutting Criteria of Model-----	66
	5.3.3 Miner’s Hypothesis to Estimate Pavement Damage-----	66
5.4	INPUTS AND RESULTS FROM WELSEA MODEL SIMULATIONS-----	67
	5.4.1 SINGLE-AXLE SIMULATION MODEL-----	67
	5.4.2 TANDEM-AXLE SIMULATION MODEL-----	68
	5.4.3 TRIDEM-AXLE SIMULATION MODEL-----	68
5.5	STUDY EXPECTATIONS-----	71
	SUMMARY-----	69
Chapter Six CONCLUSIONS AND RECOMMENDATIONS-----		70
6.1	STUDY EXPECTATIONS-----	70
6.2	CONCLUSIONS-----	70
6.3	RECOMMENDATIONS-----	72
REFERENCES-----		74
APPENDICES		
APPENDIX A Location Maps of Test Sites-----		77
APPENDIX B Operating Procedures for Dynatest KP 100 Portable FWD-----		78
APPENDIX C CR-1000 Program Code-----		87
APPENDIX D WESLEA for Windows Simulation Outputs-----		90

LIST OF FIGURES

Figure 1.1: Methodology of Assessment of Study-----	5
Figure 1.2: Com pilot, hand device connected to PFWD -----	8
Figure 1.3: Blue tooth connectivity to the PFWD-----	8
Figure 1.4: The hand PC being connected-----	8
Figure 1.5: Deflection and Force curves on the screen-----	8
Figure 2.1: Wheel Configuration of Tractor Trailer Unit-----	11
Figure 2.2: Vertical Stress Distribution-----	12
Figure 2.3: Relation between Tire and Contact Pressure-----	13
Figure 2.4: Stress Overlap due to Dual Wheels-----	15
Figure 3.1: Highway 630-Section 1 north bound, 30 test points-----	20
Figure 3.2: PFWD versus FWD, Subgrade Resilient Modulus-Highway 630-----	27
Figure 3.3: PFWD versus FWD, Subgrade Resilient Modulus-Highway 630-----	27
Figure 3.4: PFWD versus FWD, Layer Composite Modulus-Highway 630-----	28
Figure 3.5: PFWD versus FWD, Layer Composite Modulus-Highway 630-----	28
Figure 3.6: FWD versus PFWD for Deflection Do-Hwy 630-----	29
Figure 3.7: FWD versus PFWD for Deflection Do-Hwy 630-----	29
Figure 3.8: Schematic Flow Chart Exhibiting Proposed Methodology for SLR and TPCS Equipped Truck Hauling during CTI Trial conducted on Hwy 601 and 651 During Spring 2008-----	34
Figure 3.9: Test Section on Hwy 601, PFWD Testing in Progress-----	35
Figure 3.10: Hwy 601, Section 1-----	37
Figure 3.11: Hwy 601, Section 2-----	37
Figure 3.12: Hwy 601, Section 3-----	37
Figure 3.13: Hwy 601, Section 4-----	38
Figure 3.14: Hwy 601, Section 1-3 combined-----	39
Figure 3.15: Hwy 601, Section 1-4 combined-----	39
Figure 3.16: Hwy 601, all sections shown-----	40
Figure 3.17: Highway 651, Section 6-Control Section-----	41
Figure 3.18: Hwy 651, Section 1-----	42
Figure 3.19: Hwy 651, Section 2-----	43
Figure 3.20: Hwy 651, Section 2A-----	43
Figure 3.21: Hwy 651, Section 5-----	43
Figure 3.22: Hwy 651, Section 6-Control Section-----	44
Figure 3.23: Hwy 651, Section 1-6-----	44
Figure 3.24: Hwy 651, all sections shown-----	45
Figure 4.1: View of Thermistor String at Test Site-----	47
Figure 4.2: Coring for Thermistor Installation-----	47

Figure 4.3: Thermistor string Installation, Backfilled with the same material, rammed, and sealed with cold mix. (Hwy 651, Nov. 6, 2007) -----	48
Figure 4.4: The saw cut trench is ready for the string to go in, Hwy 601-----	48
Figure 4.5: Installation of CS-616, the probe is inserted into the subgrade, Hwy 651-----	50
Figure 4.6: The CS-616 probe is inserted horizontally at the sub grade level, Hwy 601-----	50
Figure 4.7: CR-1000 Datalogger-----	51
Figure 4.8: Tower mounted with Data logger Cabinet and Solar Panel, Hwy 651-----	53
Figure 4.9: Sensors installed, Tower Erected, Data logger Programmed and the set up is being tested on Hwy 651-----	53
Figure 4.10: Erection of Campbell’s Tower arrangement eliminated and the mast is being fixed to the Cabinet provided by MTO, Hwy 60-----	54
Figure 4.11: Sensors installed, connected to data logger and check-run in progress, Hwy 601-----	54
Figure 4.12: PC 400 screen demonstrating highway 601 Pavement and Air Data-----	56
Figure 5.1: Highway 601, Section 3, CTI-Trial with a TPCS equipped chip truck, May 2008-----	63
Figure 5.2: Highway 601, Section 3, CTI-Trial with a TPCS equipped chip truck, May 2008-----	63
Figure 5.3: A typical TPCS equipped logging truck on Highway 651-----	64
Figure 5.4: A loaded TPCS equipped logging truck on Highway 65, Trial May 2008-----	65

LIST OF TABLES

Table 1.1: PFWD versus FWD-----	2
Table 3.1: Summary of Field Testing on Highway 630-----	22
Table 3.2: Highway 630 Pavement Structure-----	24
Table 3.3: Averaged Pavement Layer Modulus and Resilient Modulus-----	26
Table 3.4: Averaged PFWD and FWD Deflections on Highway 630-----	29
Table 3.5: Pavement Structure of British Columbia’s MOT Low Volume Roads-----	30
Table 3.6: Highway 601 in-situ strength monitoring through repeated PFWD Testing-----	36
Table 3.7: Highway 651 in-situ strength monitoring through repeated PFWD Testing-----	41
Table 4.1: Freezing/Thawing Indices on Hwy 601 as worked out from on-site sensor readings-----	59
Table 4.2: Freezing/Thawing Indices on Hwy 651 as worked out from on-site sensor readings-----	59
Table 4.3: Implementation and Termination Dates for Reduced Loading-Northwestern Region-----	60
Table 5.1: Summary of CTI-Trial on Hwy 601 and 651-----	62
Table 5.2: Summary of Pavement Failure Results from Single-Axle Simulations-----	68
Table 5.3: Summary of Pavement Failure Results from Tandem-Axle Simulations-----	68
Table 5.4: Summary of Pavement Failure Results from Tridem-Axle Simulations-----	69

Chapter One

INTRODUCTION

1.1 RESEARCH OBJECTIVE

Roads represent the largest in-place asset value of a transport infrastructure in most countries. Keeping this asset from depreciating below some specified level while at the same time providing a desired level of service to the road users, presents a major challenge. The study is aimed at exploring a quantifiable solution to this challenge. Traffic loading, environmental conditions, subgrade soil, construction, and maintenance quality are among the various factors which influence pavement performance. Environmental conditions can have a particularly significant impact on how well pavements will perform. Pavement designers need to pay special attention to various environmental design considerations such as freeze thaw cycles, spring thaw weakening, and frost susceptible soils.

The primary goal in implementing Seasonal Load Restriction (SLR) and Winter Weight Premium (WWP) is to strike the right balance between minimizing maintenance costs associated with road damage and minimizing economic loss due to restricting weights for trucks. Start and end dates must be properly administered. Inaccurately determining either SLR or WWP may lead to premature damage and result in higher maintenance costs or reduced economic activity.

In addition to the SLR and WWP policies, there are potential technologies which can be utilized that potentially mitigate damage. The proposed approach by FERIC to minimize pavement damage during the load restricted period involves the use of the TPCS technology. TPCS is a technology that adjusts truck tire pressures to minimize the impact of axle loads on weight restricted, thin pavement roadways during the spring thaw season.

Highway 630, in Mattawa-North Bay Ontario is the preliminary test site to examine the spring thaw pavement weakening. Theoretically, reduced tire pressure should lower the potential for fatigue cracking on thin asphalt pavement structure. However, the potential to reduce the anticipated structural damage due to poor subgrade conditions, particularly for surface treated pavements, are being evaluated in this study. Past studies have shown that varying the tire inflation pressure only affects stresses at the asphalt pavement base layer. The only way to reduce the phenomenon of secondary rutting, which results from weak sub-grade, would be to reduce loads.

However, there is some consensus among pavement experts that the reduction of surface contact stresses may be beneficial in terms reducing fatigue cracking as well as the surface distress associated with the tire-pavement contact stress. There is no standard model (similar to the Asphalt Institute fatigue model) available for evaluating the ELSYM-5 computer software program in combination with the Asphalt Institute (AI) structural failure criteria which is only suitable for asphalt pavements [Tighe 2007]. Extending this analysis to surface treated pavements may not be appropriate. Secondly, this analysis relies on measured FWD deflection measurements which may not be economical for use on a routine basis either by public sector agencies or by private industry. Table 1.1 summarizes the comparison between a portable Falling weight Deflectometer (PFWD) and a trailer mounted Falling Weight Deflectometer.

Table 1.1: PFWD versus FWD

Device	Advantages	Disadvantages
PFWD	<ul style="list-style-type: none"> • Easy to use • Portable • Data easily interpreted • Follows seasonal stiffness changes in pavements 	<ul style="list-style-type: none"> • Inexpensive • Need to establish values and accuracy testing • Not very durable • Records deflection and modulus at a maximum of three sensor offsets
FWD	<ul style="list-style-type: none"> • Simulates vehicular loads with various weights • Multi-purpose pavement applications, ranging from unpaved roads to airfields. • Accurate and fast (up to 60 test points/hr). • Records deflection/modulus at maximum of nine sensor offsets. 	<ul style="list-style-type: none"> • Expensive • Requires a vehicle in addition to the instrument • Requires complex soft wares to interpret data

The use of a Portable Falling Weight Deflectometer (PFWD) is recommended to monitor the pavement strength in the spring thaw period. This validation follows through carrying out extensive PFWD testing on three test site locations. All three test roads fall under the category of Low-Volume Surface Treated Roads namely Highway 630 in Mattawa-Ontario which is also the preliminary test site, Highways 601 and 651 located in Dryden and Chapleau Ontario respectively are the two other sites that are tested and evaluated during the study. The location map for the three test sites is provided in Appendix A. The research objectives are summarized below.

- Evaluating pavement’s in-situ strength through NDT techniques and correlating Falling Weight Deflectometer (FWD) to the Benkelman Beam (BB)

- Introducing a portable and cost effective portable FWD instead of the FWD and BB
- Exploring the confidence in using the PFWD to monitor pavement strength in terms deflection and stiffness values due to seasonal variations on surface treated roads
- To help MTO in identifying true SLR period based on the results of the repeated deflection monitoring of the test sites and real time data from the use of innovative sensors
- Evaluate the effect of reduced tire pressure on pavement aiming at looking for a window to allow TPCS equipped trucks to haul with full loads during the last two to three weeks of the SLR period.

1.2 OVERVIEW

Thousands of kilometres of roads are either closed or severely restricted to heavy traffic due to structural weakness of pavement during spring thaw every year. The spring thaw period varies in length depending on the severity of the winter. As soon as thaw occurs, pavements become weak due to the high moisture content in the underlying base course and subgrade. The base course and subgrade can become completely saturated in extreme cases and even result in weakening of the pavement to such an extent that even less than one hundred passes of an 8170 Kg (18,000 lbs) axle will cause the pavement to fail. Most of the pavement structures with high traffic volumes in areas where roads are subject to freezing are designed to resist the effects of spring thaw. To achieve this, some agencies construct pavements where the depth of the pavement structure built of non-frost susceptible materials such as crushed stone bases is at least half the expected depth of freeze. This type of construction is expensive when it is seen that the depth of freeze especially in northern Ontario can be more than 1.5 metres (5 feet). Similarly other techniques used to resist the weakening caused by spring thaw usually increase construction cost.

To reduce damage during spring thaw, some road departments place load restrictions on vehicles. These load restrictions are often as much as a 50 percent reduction of normal loads [*Highway Traffic Act 1990*]. Even with these load restrictions, a large amount of money is spent each year repairing the damage caused by spring-thaw cycle.

Although the load restrictions do reduce pavement damage and reduce repair costs, these restrictions cause considerable economic impacts. Load restrictions are placed mostly on low volume roads which have not been designed nor constructed to resist the effect of spring thaw. These load restrictions can prevent transportation of goods by heavy vehicles, typically tractor semi-trailers. In many cases,

companies may have to stop some or all of their operations during this period. This results in economic losses to employees, companies, industries, provincial and local governments. Essentially any type of business that relies on the use of heavy trucks in its operations can be adversely affected when load restrictions are placed on roads due to weakened pavement.

1.3 STUDY OUTLINE

Chapter one reviews the research objective and the different tools used to assess the in-situ pavement strength.

Chapter Two reviews the effects of tire pressure, axle loads, and tire type on pavement structures. Lower tire pressures provide benefits on thin flexible pavements (less than 100 mm of asphalt concrete) or aggregate surfaced gravel roads which are typical for low volume roads. Axle loads also played the largest role in reducing stress and strains in flexible pavements. This chapter also reviews the results of three “AASHO type” closed loop roads tests and a field test conducted by the Department of Agriculture, U.S. Forest Service on CTI applications.

In Chapter Three, the methodology used to monitor in-situ pavement strength through using Non-Destructive Testing (NDT) is discussed. Conventionally the Ministry of Transportation in British Columbia and Ontario has been using the Benkelman Beam and the trailer mounted Falling Weight Deflectometer (FWD) respectively for these surveys which are considered costly. Therefore, the study aims at introducing the use of the Portable Falling Weight Deflectometer (PFWD). The PFWD can provide seasonal variations in pavement stiffness. Correlations between the Benkelman Beam (BB), the FWD and then to the PFWD are developed. Threshold values for imposing and lifting the Seasonal Load Restrictions (SLR) are derived and fixed. The use of a PFWD is recommended to monitor pavement strength in terms of deflection and stiffness for surface treated low volume roads.

In Chapter Four, the details and significance of using sensors on two of the test sites is described. It is aimed at looking for a possibility to reduce the SLR period by monitoring the exact freeze thaw cycle closely through instrumentation such as thermistor strings, soil moisture content probes, relative humidity and air temperature probes. Highways 651 and 601 in Chapleau and Dryden, Ontario are instrumented for

this purpose. Real time data is recorded at an interval of one hour. The freeze-thaw cycle is monitored on both the test highways and the results are interpreted in this chapter.

Chapter Five summarizes the analysis for reduced tire pressure and full axle loads. The results of a theoretical investigation of the effects of lower tire pressure on roads in a severely weakened condition, such as is found during spring thaw. With the recent technology development of Central Tire Inflation (CTI) in the trucking industry, trucks may be able to operate on roads subject to load restrictions. CTI would allow trucks to operate at lower tire pressures on load restricted roads and then easily increase tire pressure from inside the truck cabin when the truck transfers to a road not subject to load restrictions. Three different models, with different axle configuration, and tire pressures are simulated using mechanistic pavement design software to look in to the scenarios. The results are interpreted in this chapter

1.4 SCOPE OF STUDY

Figure 1.1 outlines the methodology of assessment of the study.

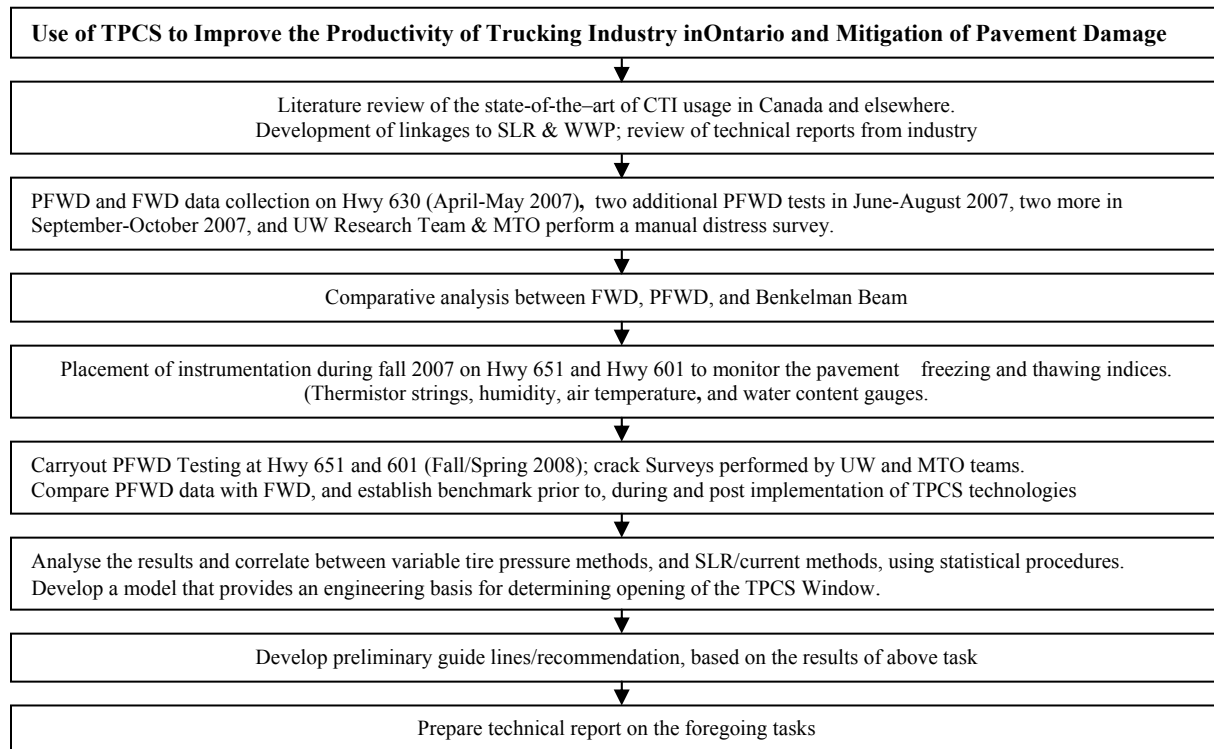


Figure 1.1: Methodology of Assessment of the Study.

To fulfill the proposed approach, to realize the objectives, and to be able to achieve continuity with the research team, a two year frame was necessary. Most importantly, the two year period allowed the team to compare behaviors; with both time and climatic conditions at a given set of loading patterns.

Phase 1, which was completed jointly by the Forest Engineering Research Institute of Canada (FERIC) and the Ministry of Transportation Ontario (MTO) on the project, successfully demonstrated the use of TCPS technology. It will be necessary to review on a commercial basis. Moreover, Highway 630 was surveyed for visible distresses only in the absence of any in-ground sensors, Road Weather Information System (RWIS) and weather related data.

In order to validate and develop an adoptable strategy towards allowing CTI/TPCS use commercially in Northern Ontario, with more insight and knowledge of pavement conditions; this study has accounted for all relevant parameters like the behavior of different pavement layers with changing weather conditions. This has enabled the research team to establish benchmarks using the Portable Falling Weight Deflectometer which has compatible results with the Falling Weight Deflectometer (FWD).

The PFWD has shown good reliability for seasonal stiffness variations and can be compared well with FWD on asphalt surfaces [*Steinert 2005*]. The basic approach in this study is to identify and quantify the potential effectiveness of the use of PFWD for surface treated roads with specific application to monitoring CTI/TPCS on Northern Ontario's roads.

Literature review on the state-of-art of Central Tire Inflation (CTI) usage and current activities in Canada has provided an independent overview of the usage of the technology [*Bulley 2001*]. The application of CTI usage and literature available has been analysed and updated, and linkage to Seasonal Load Restrictions (SLR) has been developed. The study is aimed at quantifying the strength of the existing pavement using PFWD and FWD data. Following this validation, the effect of various tire pressures on surface treated roads is being evaluated and thresholds for performance being established, which wherein after will be set as guidelines for adoption by users and agencies.

1.5 FIELD TESTING

The Portable Falling Weight Deflectometer (PFWD) is used to monitor the behavior of the spring thaw weakened pavement. The PFWD has shown promise as a tool for seasonal stiffness measurements and can be compared well with FWD on asphalt surfaces [Steinert 2005]. The approach is to identify and quantify the potential effectiveness of the use of PFWD for surface treated roads in Canada.

The Falling Weight Deflectometer (FWD) is a device capable of applying dynamic loads to the pavement surface, similar in magnitude and duration to that of a single heavy moving wheel load. The response of the pavement is measured in terms of vertical deformation, or deflection, over a given area using seismometers. Thus, the use of FWD enables for the determination of a deflection basin caused by a controlled load. FWD generated data combined with layer thickness, can be confidently used to obtain the ‘in-situ’ resilient elastic modulus of a pavement structure. The two common types of FWDs used in data collection are the Portable Falling Weight Deflectometer (PFWD) and the trailer mounted Falling Weight Deflectometer (FWD). The FWD although efficient is expensive and time consuming thus the PFWD offers same benefits.

1.6 PORTABLE FALLING WEIGHT DEFLECTOMETER (PFWD)

The PFWDs used in this study are owned and operated by the Centre for Pavement and Transportation Technology (CPATT) at the University of Waterloo are the Dynatest KPI 100 and LWD 3031, which were used extensively for deflection data collection. FERIC has also used a similar instrument for the same purpose. The portable Falling Weight Deflectometer PRIMA100 - FWD is a handy instrument for on-site measurement of bearing capacity to minimize risks and optimize quality. The Portable Falling Weight Deflectometer (PFWD) was investigated as a tool to aid in determining when to impose weight restrictions on low-volume roads during the spring thaw [Kestler, 2005].

The Dynatest KPI 100 or LWD 3031 PFWD equipment enabling high quality data collection is very low in cost and means of tremendous cost reduction as on-site analysis of collected data allows immediate information. Site locations can be captured by means of GPS (Geographic Positioning System), which enable presentation of data in maps or general plans of the site. The data transfer system of the new generation of PFWD is very flexible and allows for wireless transfer of data. The Dynatest’s portable

FWD is powered by four 1.5 volt standard AA batteries and no extra power supply is needed. The Dynatest standard model has one centre geophone. Moreover, PFWDs directly measure the stiffness of pavement systems and compacted layers which is needed for mechanistic pavement design. The results of the first drop should always be neglected since the first weight drop helps in ensuring proper seating of the base plate. It is recommended that the results from drops two through six be averaged to obtain results that are representative of a test location [Kestler 2005].

1.7 PFWD TESTING PROCEDURE

The PFWD equipment is assembled and it is connected to the com pilot-palm device, through Bluetooth. The connectivity is checked through the blinking green light. Each point in a selected test section is tested six times. The first reading is discarded and average of the remaining five readings is taken into consideration [Kestler 2005]. Figure 1.2, 1.3, 1.4, and 1.5 illustrates the display screen of the handheld com pilot. The PFWD Operation Procedures developed by CPATT at the University of Waterloo are annexed in Appendix B.

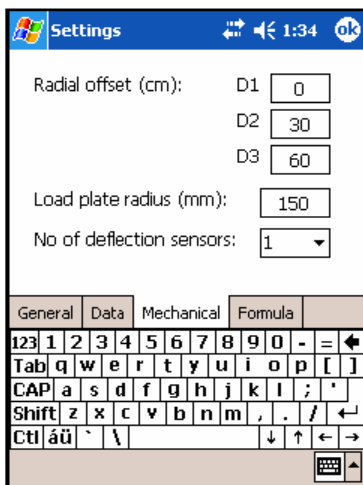


Figure 1.2: Com pilot, hand device connected to PFWD

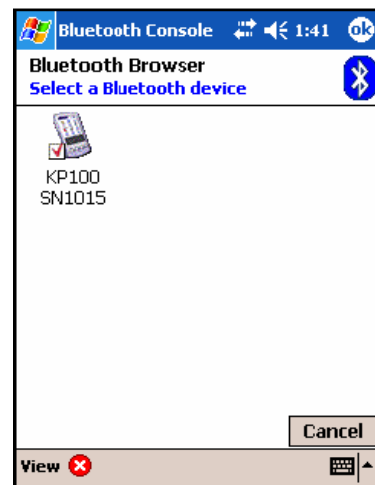


Figure 1.3: Blue tooth connectivity to the PFWD

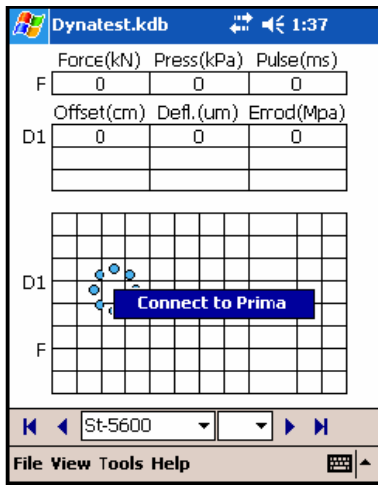


Figure 1.4: The hand PC being connection

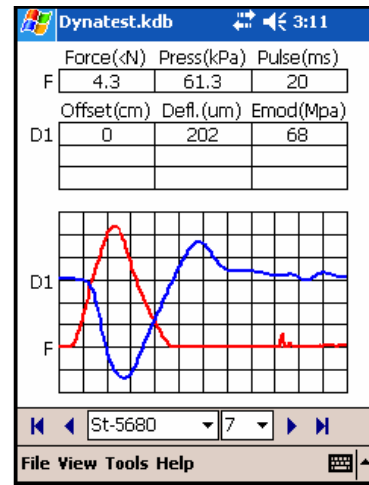


Figure 1.5: Deflection and Force curves

1.8 FALLING WEIGHT DEFLECTOMETER (FWD)

The FWD is a Nondestructive Deflection Testing (NDT) device for use in pavement structural evaluation. The Falling Weight Deflectometer (FWD) is a readily available, industry-accepted testing instrument that measures the pavement response (i.e., deflection) to a load that simulates the in-service truck loads applied to the pavement. The FWD is a multifunctional tool that can be used in various facets of a pavement project. In addition to its conventional, well-established use for evaluating pavement condition, FWD testing (and the associated analysis) can also be used to identify the factors that affect pavement condition and to monitor the effectiveness of pavement rehabilitation efforts [Frabizzio 2002].

The FWD applies a dynamic load through a circular plate that is lowered to the pavement surface. Sensors in contact with the surface measure the downward deflection of the pavement surface. This deflection bowl is then used to assess the structural condition and to identify weaknesses in any of the pavement layers. The primary function of the FWD is to provide deflection data for evaluating the in-situ structural condition of pavement structures. A complement of FWD testing and other test methods provides the necessary information for evaluating pavement condition in a reliable, mechanistic manner. When testing is conducted away from cracks and joints, FWD data can be used to determine the elastic modulus of the various pavement layers. The NDT technique through using the FWD has gained popularity because it can assess structural integrity and estimate the elastic modulus of in-place pavement systems [Wu 2006].

Chapter Two

LITERATURE REVIEW

2.1 EFFECT OF TIRE PRESSURE ON PAVEMENT STRUCTURE

The thickness of a pavement primarily depends upon the design wheel load. Higher wheel loads require thicker pavement structures as compared to lower wheel loads, provided other design factors such as subgrade soil, climatic factors, pavement component materials, and environmental factors are the same. While considering the design wheel load, the effect of static wheel loads, multiple wheel load assembly (if any, like the dual or the dual-tandem wheel loads), contact pressure, load repetition and the dynamic effects of transient loads are to be taken into account. As the speed increases the rate of application of the stress is also increased resulting in a reduction in pavement deformation under the load; but on uneven pavements, the impact increases with speed.

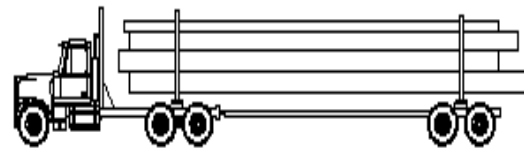
The various wheel load factors to be considered in pavement design and maintenance are explained in the following sections.

2.2 MAXIMUM WHEEL LOAD

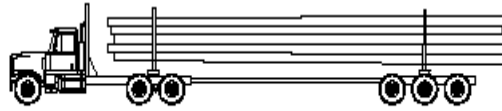
The wheel load configurations are important in order to know the way in which the loads of a given vehicle are applied on the pavement surface. Typical wheel load configurations of a tractor trailer unit are shown in Figure 2.1 [Oliver 2004].

For highways the maximum legal axle load as specified by AASHTO is 8170 Kg (18000 lbs) with a maximum equivalent wheel load of 4085 Kg (9000 lbs). Total load influences the thickness requirements of the pavements.

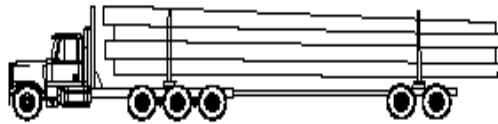
Previous studies show that axle configuration play a minor role in pavement performance. Only one study by Sebaaly addressed this factor [Sebaaly 1992]. The study found that multiple axles produce lower tensile strains but higher compressive stresses than single axles under the same per axle load.



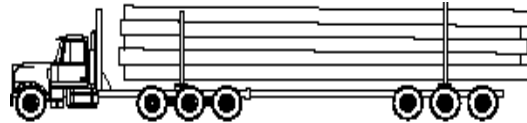
Tandem tractor / Tandem pole trailer



Tandem tractor / Tridem pole trailer



Tridem tractor / Tandem pole trailer



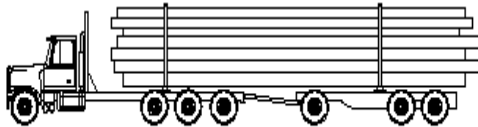
Tridem tractor / Tridem pole trailer



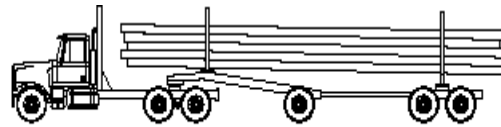
Tandem tractor / Quad axle trailer



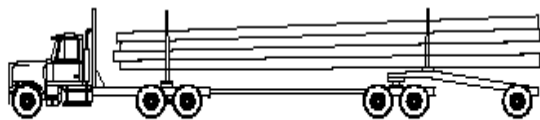
Tandem tractor / Triaxle trailer



Tridem tractor / Triaxle trailer^f



Tandem tractor / Jeep / Pole trailer



Doglogger



Tandem tractor / Tandem jeep / Pole trailer

Figure 2.1: *Wheel Configuration of Tractor Trailer Unit*

2.3 WHEEL LOAD AND TIRE PRESSURE

Tires influence the quality of the surface (wearing) coarse. In fact, the magnitude of the vertical pressure at any depth of soil subgrade or pavement section depends upon the surface pressure as well as on the total wheel load.

The equation for vertical stress computations under a uniformly distributed circular load based on Boussinesq's theory is given by [Khanna 1999]:

$$\sigma_z = q \left[1 - \frac{z^3}{(a^2 + z^2)^{3/2}} \right] \quad (2.1)$$

Here

σ_z = Vertical stress at depth z ,

q = Surface pressure or contact pressure, and

a = Radius of loaded area.

Using the above equation, the variation of vertical stress σ_z with depth is plotted as given in Figure 2.2.

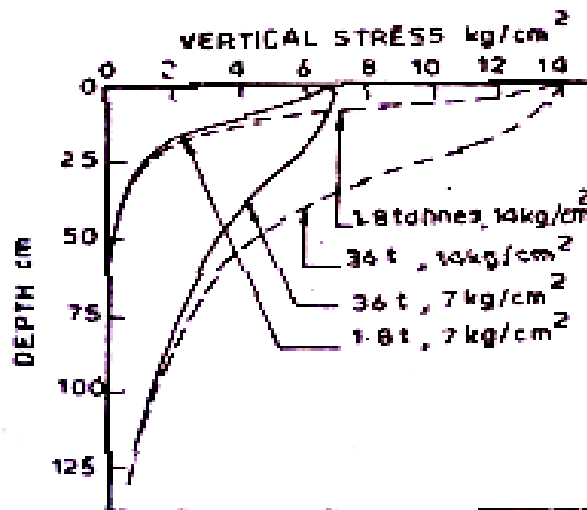


Figure 2.2: Vertical Load Stress Distribution [Khanna 1999]

As seen from Figure 2.2, the influence of tire pressure is predominating in the upper layers. At a greater depth, the effect of tire pressure diminishes and the total load exhibits a considerable influence on the vertical stress magnitudes. Tire pressure of higher magnitudes therefore demand high quality materials in the upper layers in pavements. The total depth of pavement is, however, not influenced by tire pressure. With constant tire pressure, the total load governs the stress on the top of the subgrade within allowable limits.

Figure 2.2 also implies that a narrow concentrated rolling load such as that of a horse driven cart will produce very high stresses at the pavement surface. This demands the use of very strong and hard

aggregates for the wearing surface to resist damage. However, the stresses at a lower level of the cart wheel are negligibly small as the gross load is very small.

Generally, the wheel load is to be distributed over a circular area. But through many measurements of the tire imprints with different load and inflation pressure, it is seen that the contact areas in many cases are elliptical in shape in many cases. Three important terms related to tire pressure are *tire pressure*, *inflation pressure*, and *contact pressure*.

Theoretically, all these terms are equivalent. Tire pressure and inflation pressure mean exactly the same thing. The contact pressure is found to be more than tire pressure when the tire pressure is less than 7 Kg/cm² (100 psi) and is vice versa when the tire pressure exceeds this value. The general variation between the tire pressures and the measured contact pressure is shown in Figure 2.3.

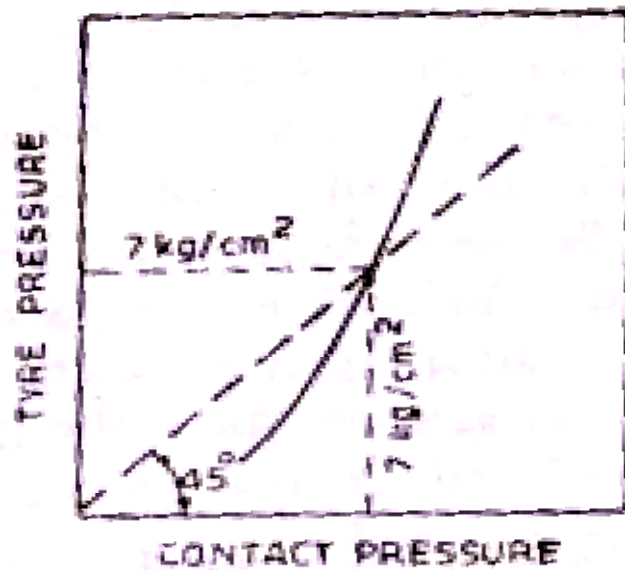


Figure 2.3: Relation between Tire and Contact Pressure

Contact pressure can be measured by the relationship given below.

$$\text{Contact Pressure} = \frac{\text{Load on the wheel}}{\text{Contact Area or area of imprint}} \quad (2.2)$$

Where Contact Pressure is measured in units of pressure Kg/cm^2 or lb/in^2 , load on the wheel is expressed in Kilograms or pounds, and contact area is denoted in in^2 or cm^2 .

The ratio of contact pressure to tire pressure is defined as Rigidity Factor (RF). An RF value of 1.0 would be the typical average tire pressure of 7 Kg/cm^2 . This value is higher than unity for lower tire pressure and less than unity for tire pressure higher than of 7 Kg/cm^2 . The Rigidity Factor (RF) depends upon the degree of tension developed in the walls of the tires.

Tire contact pressure is the actual pressure measured where the tire contacts the pavement surface. Three assumptions are usually made regarding tire contact pressure in most pavement response studies. These include tire pressure is uniform; it acts on the circular area, and it is equal to the tire inflation pressure. This simplified theoretical analysis is believed to be of sufficient accuracy for design work. However, premature failure of some pavements designed according to these assumptions can cause an underestimation of the strains and stresses due to truck tire loading in those studies [Roberts 1986].

The correlation between inflation pressure and actual contact pressure is one area of tire performance that is not well understood. Due to the many different types of tires and their construction, a reliable model has not been developed to predict actual tire contact pressure. Analytical studies of truck tires show that the contact pressure can be two times the inflation pressure where the tire contacts the road surface. Tire inflation pressures of 75 psi (517 kPa) and 125 psi (862 kPa) resulted in peak contact pressures of 150 psi (1034 kPa) and 220 psi (1517 kPa) respectively [Roberts 1986]. The scope of the Roberts study was expanded when it was found that the basic assumption that tire/pavement contact pressure is equal to the tire inflation pressure was in error. Roberts did find that at a constant tire load, the tire contact pressure becomes more uniform at lower tire pressures.

2.4 EQUIVALENT SINGLE WHEEL LOAD (ESWL)

To carry a greater load while keeping the maximum wheel load within the specified limit, and to carry greater loads, it is necessary to provide wheel assembly to the rear axles of the load vehicles. In doing so the effect on the pavement through a dual wheel assembly is obviously not equal to two times the load on any one wheel. In other words, the pressure at a certain depth below the pavement surface cannot be

obtained by numerically adding the pressure caused by each wheel load. The effect is in between the single load and two times the load carried by any one wheel.

The clear distance between the inner edges of the tires, divided by two ($d/2$), as shown in Figure 2.4, each wheel load acts independently and after this point the stress induced due to each load begins to overlap. At depth $2S$, where S is the distance from tire centre to tire centre, shows the stresses induced are due to the effect of both wheels as the area of overlap is considerable. So the total stresses due to the dual wheel at any depth greater than $2S$ is considered to be equivalent to a single wheel load of magnitude $2P$, where P is the load on the single wheel, though this stress is likely to be slightly greater than the stress due to the wheels.

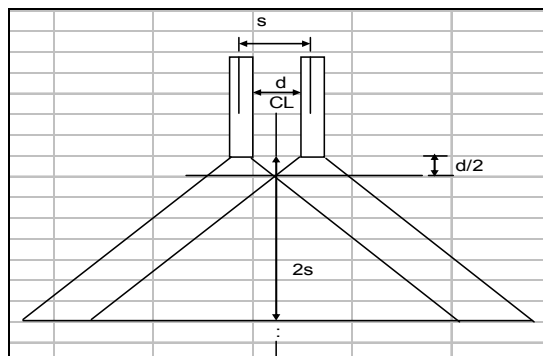


Figure 2.4: *Stress Overlap due to Dual Wheels*

Suppose a dual wheel load assembly causes a certain value of maximum deflection D_0 at a particular depth Z (say, depth equal to the thickness of the pavement). As per deflection criterion, the Equivalent Single Wheel Load (ESWL) is that single wheel load having the same value of maximum deflection at the depth Z . Similarly, by stress criterion, the ESWL is the single wheel load producing the maximum stress at the desired depth Z as the dual.

2.5 TIRE PRESSURES AND PAVEMENT PERFORMANCE

The effects of tire pressure on pavement performance with regards to fatigue and rutting failure depends generally on two pavement properties: pavement thickness and stiffness of the base and subgrade layers.

2.5.1 PAVEMENT THICKNESS

In the studies reviewed, asphalt pavement thickness ranged from 25 mm to 250 mm. With regards to fatigue failure, when asphalt concrete pavement thickness is in excess of 100 mm, the effects of tire pressure on tensile strains were found to be relatively minor. Roberts found that for asphalt concrete pavement thicknesses of 100 mm or greater, the effect of tire inflation pressure on tensile strains was less than ten percent, while Sebaaly reached the same conclusion noting that the effect of inflation pressure was as low as one percent for asphalt layers with thicknesses of 100 mm, 150 mm, and 300 mm [Sebaaly 1992].

2.5.2 STIFFNESS OF BASE AND SUBGRADE

The stiffness of the base course has been found to have an effect on the amount of influence tire inflation pressure had on strains. Roberts showed that increasing tire inflation pressure from 75 to 125 psi produced a range of 20 to 30 percent increase in the tensile strain for a 25 mm (one inch) surface. This was supported by results from an analytical study which found an approximate 35 percent increase in tensile strain by increasing the inflation pressure from 517 kPa (75 psi) and 862 kPa (125 psi) for the same thickness [Marshek 1985]. The reason for the range of a 20 to 30 percent increase in the tensile strains in the Roberts study was determined to be a function of the base course stiffness. The stiffest base course (Elastic modulus equal to 414 MPa or 60,000 psi) caused a 30 percent increase in tensile strain at the bottom of asphalt while the least stiff (elastic modulus equal to 138 MPa or 20,000 psi) caused a lower increase of 20 percent. However, the range of base course stiffness used in the study (elastic modulus equal to 138 MPa or 20,000 psi to 414 MPa or 60,000 psi) was relatively stiff compared to values found during spring thaw [Lary 1984, Sebaaly 1992]. No studies analyzing the effects of weak bases and tire inflation pressure on pavement strains were found.

The effect of tire pressure on rutting failure, which is a function of compressive strain, is minimal in the cases studied. Marshek reported that increasing tire inflation pressure from 517 kPa (75 psi) and 862 kPa (125 psi) in asphalt pavements 50 to 100 mm thick produced only a small increase in the compressive strains at the top of subgrade for the cases modeled. Therefore, they concluded that tire inflation pressure was an insignificant factor in causing subgrade rutting [Marshek 1985]. However, this study only examined the effects of a single tire load, thereby omitting the effects of multiple tire loads.

2.5.3 AXLE LOADS

In the studies reviewed, axle load was found to be directly related to both fatigue and rutting failure. Marshek found that increasing loads resulted in increases in both horizontal tensile strain and horizontal shear strain in the asphalt course. Therefore, he has concluded that of all the factors studied related to fatigue failure, axle load was the primary factor causing fatigue failure [Marshek 1985].

Axle load was found in several studies to be related to vertical compressive strain. Sebaaly observed that the effect of the axle load on the compressive strains in the subgrade was relatively uniform for all asphalt concrete surface thicknesses. Any increase in the axle load increased the maximum compressive strain by a proportional amount, regardless of asphalt thickness. *Sebaaly* noted that a twenty percent increase in axle load produced a twenty percent increase in the critical subgrade compressive strain for the 50 to 250 mm thickness of asphalt concrete in the study [Sebaaly 1992]

2.5.4 AXLE CONFIGURATION

Axle configuration was found to play a minor role in pavement performance [Sebaaly 1992]. The study found that tandem axles produce lower tensile strains but higher compressive stresses (vertical compressive strains were not reported) than single axles under the same per axle load. For example a load of 7985 Kg (17600 lbs) on a single axle (total load 7985 Kg or 17600 lbs) produced a horizontal tensile strain of 145 micro strains at the bottom of the asphalt layer, while a load of 7800 Kg (17,200 lbs) per axle on a tandem axle (total load 15610 Kg or 34,400 lbs) produced only 133 micro strains. Compressive stress for the same loading conditions was found to be 39 kPa (4.2 psi) for the single axle and 46 kPa (6.9 psi) for the tandem axle. The reason for this is explained by the pavement tensile strain response. When the pavement structure is subject to a tandem-axle load, the axle on top of the point of interest produces horizontal tensile strains while the axle 50 inches away produces horizontal compressive strain. Therefore, a portion of the tensile strain is cancelled by the compressive strain. In the case of the of the single-axle configuration, the point of interest is only subjected to tensile strain, and no cancelling effect occurs. Therefore, the tandem-axles compared with single-axles on the basis of similar pre-axle load levels, the passage of one tandem axle produces less fatigue than the passage of two single axles. Because tandem axles do not have any cancelling effects under compression, they produce higher compressive strains than single axles on an equal per axle load [Sebaaly 1992].

2.6 CENTRAL TIRE INFLATION STUDIES

The following sections describe a few studies reviewed that were conducted by various agencies on the Central Tire Inflation (CTI) phenomenon.

2.6.1 United States Federal Highway Administration Study

The United States Federal Highway Administration (FHWA) conducted a study using the Accelerated Loading Facility test machine and investigated the effects of tire pressure on flexible pavements. The first part of the two part study measured actual surface deflections and strains for different combinations of loads and tire pressure using in-place monitoring equipment. The second part of the study evaluated the extent of rutting and fatigue cracking on two pavement test sections using the same load but different tire pressures after 100,000, 200,000, 300,000, 400,000, 500,000, and 600,000 passes of a simulated load.

From the data in part one, it was concluded that the effects of tire pressure on the tensile strain was very small. The range of increased tensile strain measurements for a constant tire load and increased tire pressures was from two to ten percent.

The second conclusion reached from the first part of the study was that axle load played a significant role in the magnitude of the tensile strains. In this study, increasing the load from 4265 Kg (9,400 lb) to 8620 Kg (19,000 lb) resulted in an increase of 200 to 400 percent in the measured tensile strain at the bottom of the asphalt concrete.

The second part of the study was designed to measure the effects of tire pressure on fatigue cracking and rutting. The results indicated that lower tire pressure does increase pavement life when considering both fatigue and rutting criteria.

2.6.2 Tire Type

Although there is limited information available on this, the type of tire does play a small role in pavement response and performance. One study by Sebaaly compared the effects of four different types of tires on pavement response [Sebaaly 1992]. The in-situ horizontal tensile strains were measured for each tire type. The pavement was subjected to identical axle loads of 8,000 kg (17,600 lbs)

on single axle, 9,800 kg (21,600 lbs) on a single axle, 7900 kg (17,400 lb) per axle on a tandem axle, and 6670 kg (14,700 lb) per axle on a tandem axle. The tensile strain was measured for each tire type which included dual tires, 11R22.5 inflated to 724 kPa (105 psi) and 827 kPa (120 psi), 385/65R22.5 single tire at 827 kPa (120 psi), and 425/65R22.5 single tire at 827 kPa (120 psi). Passes were made at a speed of 67 km/h (40 mph). Sebaaly converted the strain measurements made to Load Equivalency Factors (LEF). Comparing the changes in the LEF, Sebaaly concluded that:

- Tire type has a significant effect on the LEF of an axle load and configuration
- Single wide-base tires have LEFs 1.5 to 1.7 times higher than dual tires for any given pavement thickness for both fatigue and rutting
- The effect of tire type on the LEF was uniform throughout the range of asphalt thickness used in the study.

2.6.3 Tests Conducted by Department of Agriculture, US Forest Service

The U.S. Army found that lowering tire pressures on low speed, unpaved roads had several potential benefits such as reduced road maintenance, reduced road surfacing requirements, reduced drive over fatigue and injury, reduced vehicle operation costs, and increased vehicle mobility [Taylor 1987].

SUMMARY

In summary, tire pressure plays a significant role in pavement fatigue performance if the asphalt concrete thicknesses were less than 100 mm (4 in) Thus, tire pressures also have a considerable effect on surface treated roads where the thickness is below 100 mm. The effect of axle configuration on tensile strain is minor, but is evident regardless of asphalt thickness. Changes in tire pressure were found to have little or no effect on pavement compressive strains regardless of the pavement thickness. The predominant factor found affecting pavement performance with regard to both fatigue and rutting failure was axle load.

Chapter Three

IN-SITU PAVEMENT STRENGTH MONITORING AND CORRELATIONS

3.1 CALIBRATION TEST SITE

The primary initial test site in this study is located on Highway 630 near Mattawa which is approximately 45 kilometres east of North Bay. This site was selected as it was tested previously in Phase 1 of the study carried out by FERIC and MTO during 2005/2006. During the time period, in May and November 2005, FWD tests were carried out in addition to the CTI testing. Figure 11 in Appendix A shows a map indicating the general location.

3.2 TEST SECTIONS

At the highway 630 site, six sections are selected in a length of about nine kilometers. Sections are selected and laid out jointly with FERIC. Sixty points were marked at an interval of three meters in each section as shown in Figure 3.1; with a total of 30 points each in the north and south bound lanes.



Figure 3.1: *Highway 630-Section 1 north bound, 30 test points*

3.3 PFWD TESTING PROCEDURES

The PFWD equipment was assembled and connected to the com pilot palm device, through Bluetooth. The PFWD procedure that has been developed for the Centre for Pavement and Transportation Technology is provided in Appendix B. The connectivity is checked through the blinking green light. Each point in a selected test section is tested six times. The first reading is discarded and average of the remaining five readings is taken into consideration [Kestler 2005].

3.4 Testing Period

To monitor the behaviour of the pavement during the spring thaw weakening conditions, Highway 630 was tested on the following days.

Day 1, April 19, 2007

Day 2, April 23, 2007

Day 3, April 30, 2007

Day 4, May 7, 2007

Day 5, May 14, 2007

The variation in strength was then related to the weather conditions.

3.5 Testing Pattern

At this location, the north bound lane is tested on every section each testing day, while the south bound lane is tested periodically and not necessarily at every visit. This testing pattern has been adopted to be representative of the pavement loading and structural behaviour. The loaded trucks haul on the north bound lane of the highway.

3.6 Data Collection

During the PFWD data collection both, pavement deflection and the modulus of elasticity (E) have been recorded for the April 2007 and May 2007 testing period. Testing was coordinated with FERIC so that both PFWD devices tested on the initial day of April 19, 2007. This has enabled the research team to look at the validation of PFWD data in conjunction with FERIC's data. Subsequent testing was carried out only with the PFWD.

Applied Research Associates (ARA) was commissioned under this study to carry out Falling Weight Deflectometer (FWD) testing on two occasions and the CPATT PFWD also took readings on those days. ARA's testing occurred on April 23 and May 7, 2007. Hence, a significant amount of deflection data has been collected on Hwy 630 during the spring thaw weakening period. This allowed the research team to examine differences in various PFWD devices also difference between PFWD and FWD. The data collection pattern has been summarized in the following Table 3.1.

Table 3.1: *Summary of Field Testing on Highway 630*

Date	Section	Direction	UW PFWD	FERIC's PFWD	ARA's FWD
April 19, 2007	1	NB,SB**	√	√	
	2	NB,SB	√	√	
	3	NB	√	√	
	4	NB	√	√	
	5	NB	√	√	
	6	NB	√	√	
April 23, 2007	1	NB	√		√
	2	NB	√		√
	3	NB	√		√
	4	NB	√		√
	5	NB	√		√
	6	NB	√		√
April 30, 2007	1	NB	√		
	2	NB	√		
	3	NB	√		
	4	NB,SB	√		
	5	NB,SB	√		
	6	NB,SB	√		
May 7, 2007	1	NB,SB	√		√
	2	NB,SB	√		√
	3	NB,SB	√		
	4	NB	√		√
	5	NB	√		√
	6	NB	√		√
May 14, 2007	1	NB	√		
	2	NB	√		
	3	NB	√		
	4	NB	√		
	5	NB	√		
	6	NB,SB	√		

* North Bound Lane, ** South Bound Lane

3.7 CORRELATION BETWEEN PORTABLE FALLING WEIGHT DEFLECTOMETER (PFWD), FALLING WEIGHT DEFLECTOMETER (FWD), AND BENKELMAN BEAM (BB)

If the PFWD was to be adopted in this work, it was necessary to validate how reliable it is and how it compared to the sturdier, robust FWD, and the Benkelman Beam which has been used for several years. The PFWD is portable and can be easily transported to reach locations. Thus, it was necessary to correlate PFWD and FWD with respect to both deflection and moduli values. The Department of Transportation (DOT) in British Columbia, Canada is evaluating the pavement structure through the wide use of the Benkelman Beam with readings of 1.5 mm to 1.25 mm in order to impose and lift the SLR during the spring-thaw period. The Benkelman Beam records deflection due to the application of static loads and does not simulate vehicular rolling load. In addition, the use of Benkelman Beam is very costly whereas the FWD is cost effective and its advantage of simulating vehicular rolling load supersedes the use of the Benkelman Beam. Besides using the FWD, CPATT has proposed the use of PFWD instead of the FWD due to the following advantages.

- Easy to use
- Portable
- Data easily interpreted
- Follows seasonal stiffness changes in pavements
- Cost effective

Hence, an attempt has been made to correlate the PFWD to the Benkelman Beam and to the FWD device to monitor and evaluate the pavement stiffness similar to B.C's threshold deflection values for imposition and lifting of the SLR in Northern Ontario. A correlation has already been established by Washington State DOT Materials Laboratory in 1982 between the BB and FWD. However, the relationship between PFWD to BB and PFWD to FWD has not been carried out. Highway 630 in Mattawa North Bay was initially tested on two different days using the FWD and PFWD. The road consists of six test sections where each section has 30 points at intervals of 3 metres. Linear correlations are developed between the two devices for both deflection and elastic/composite modulus by taking the average of the two days. Table 3.2 summarizes the pavement structure details.

Table 3.2: Highway 630 Pavement Structure

Section	Surface	Upper	Granular	Lower	Granular (mm)	Total
---------	---------	-------	----------	-------	---------------	-------

	Treatment (mm)	Binder Layer (mm)	Base (mm)	Binder Layer (mm)	Granular A 'Base' (mm)	Granular 'B' Subbase (mm)	Total (mm)	Pavement Thickness (mm)
1	30			110	270		270	410
2	60		300	80	390	170	560	1000
2	20	80	250	60	210		210	620
3	20	110	150	140	100		100	520
4	40		210	70	430	250	680	1000
5	70				170	370	540	610
6	20		180	100	310		310	610

3.7.1 FALLING WEIGHT DEFLECTOMETER (FWD) VERSUS PORTABLE FALLING WEIGHT DEFLECTOMETER (PFWD)

The following equations based have been derived based on regression analysis and collected deflection tests conducted on Highway 630 near Mattawa-Ontario. The tests were conducted on April 23, 2007 and May 7, 2007. The results are averaged for both deflection and modulus values. Equation 3.1 represents deflection while equation 3.2 represents the modulus of elasticity. The respective R² values for equation 3.1 and 3.2 are 0.73 and 0.60 respectively.

$$[FWD]_{D_0} = 3.002 [PFWD]_{D_0} - 315.55 \quad (3.1)$$

$$[FWD]_{E_0} = 1.7991 [PFWD]_{E_0} - 33.6955 \quad (3.2)$$

3.7.2 BENKELMAN BEAM TO FWD

According to the Washington State DOT Materials Laboratory study [WDOT 1982], the following relations are being used for correlating the Benkelman Beam with the Falling Weight Deflectometer.

$$BB = 1.33269 + 0.93748 [FWD]_{D_0} \quad (3.3)$$

Where BB = Benkelman Beam Deflection (inches x 10⁻³)

FWD = FWD centre-of-load deflection (inches x 10⁻³)

Based on the restrictions of a BB of 1.5 mm during spring thaw, the corresponding deflection values for FWD are calculated as follows.

$$BB = 1.5 \text{ mm} = 1.5 / (10 \times 2.54) = 0.059 \text{ inches} = 59 \text{ inches} \times 10^{-3}$$

Inserting this value of BB in Equation 3,

$$59 \times 10^{-3} = 1.33269 + 0.93748 [\text{FWD}]_{D_0}$$

$$\text{Or } [\text{FWD}]_{D_0} = 61.5131 \text{ inches} \times 10^{-3}$$

Converting (inches $\times 10^{-3}$) into (mm $\times 10^{-3}$),

$$[\text{FWD}]_{D_0} = 1562.4327 \times 10^{-3} = 1562.43 \text{ (um)}$$

3.7.3 BENKELMAN BEAM TO PFWD

In terms of BB deflection (D_0) of 1.5 mm, which appears to be a good starting point for evaluation, the corresponding deflection for the PFWD is calculated as follows.

According to Equation 3.1,

$$[\text{FWD}]_{D_0} = 3.002 [\text{PFWD}]_{D_0} - 315.55$$

$$\text{Inserting the value of } [\text{FWD}]_{D_0} = 1562.4 \text{ (um)} = 1.56 \text{ mm}$$

$$[\text{PFWD}]_{D_0} = 625.57 \text{ (um)} = 0.62 \text{ mm}$$

Similarly the corresponding PFWD value with the BB value of 1.25 mm for lifting the SLR is calculated to be 500 um or 0.50 mm.

Resultantly, the above correlations indicate that for a BB value of 1.5 mm deflection, the corresponding value of FWD deflection should be 1.56 mm, and that of the PFWD should be 0.62 mm. Therefore, 1.5 mm of BB deflection = 1.5 mm of FWD deflection = 0.6 mm of PFWD deflection. The PFWD threshold value for imposition of SLR has been adjusted to a lower value in a later section in order to accommodate the structural adequacy of Low Volume Surface Treated roads in Ontario

3.8 LINEAR REGRESSION MODEL BETWEEN FWD AND PFWD

This section outlines the correlation between FWD and PFWD for three parameters – subgrade resilient modulus, layer composite modulus, and deflection. Table 3.3 summarizes values of the pavement composite layer modulus (E_o), and Resilient Modulus (M_R) of subgrade for Highway 630 on April 23, 2007 and May 7, 2007. The composite layer modulus (E_o) is recorded directly from the FWD or PFWD data while the values for resilient modulus of the subgrade are derived through back calculation as described in AASHTO Guide for Design of Pavement Structures [AASHTO 1993]

Figures 3.2 and 3.3 demonstrate the correlation between the FWD and PFWD’s resilient modulus M_R . The R-squared value for M_R between the two devices on April 23, 2007 is 0.62 and it is 0.38 on May 7, 2007. Although this seems low, particularly for the May 7, 2007 data, these values are comparable with other studies for thin asphalt surface treated roads [Kestler 2005]. The reason behind this is the fact that the FWD which has the capacity of simulating heavier vehicular loads (40-80 KN) indicates a representative value of the subgrade modulus. On the other hand the PFWD which is sometimes also called the Light Weight Deflectometer (LWD) can simulate loads from 15 -20 KN. Thus, variation can be attributed to the difference in loading response and particularly when the pavement structure is coming out of the thaw period and is very moist.

Figures 3.4 and 3.5 demonstrate a similar linear correlation for layer composite modulus with R-squared values of 0.47 and 0.62 for the data recorded on April 23, 2007 and May 7, 2007. Equation 1 is derived by averaging the two linear models shown in Figures 3.2, 3.3, 3.4, and 3.5.

Table 3.3: Averaged Pavement Layer Modulus and Resilient Modulus

SECTION	April 23,2007				May 7, 2007			
	PFWD M_R (MPa)	FWD M_R (MPa)	PFWD E_p (MPa)	FWD E_p (MPa)	PFWD M_R (MPa)	FWD M_R (MPa)	PFWD E_p (MPa)	FWD E_p (MPa)
1	24	28	151	302	27	23	151	320
2	25	24	151	228	26	17	157	268
3	21	15	127	141	24	15	143	234
4	18	14	110	125	18	11	112	177
5	20	14	120	134	21	13	113	215
6	21	16	171	195	29	20	180	283

Six sections of road are selected in a length of about nine kilometres. Sections are selected and laid out jointly with FERIC. Sixty points are marked at intervals of 3 meters in each section as shown in Figure 3.1; a total 30 points each in north and south bound. The two devices used were CPATT's Dynatest KPI 100 PFWD and Applied Research Associate's trailer mounted FWD.

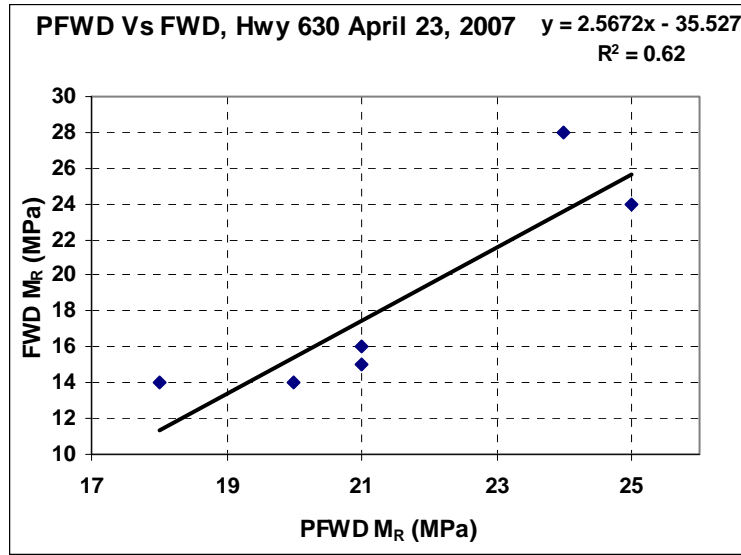


Figure 3.2: PFWD versus FWD, Subgrade Resilient Modulus-Highway 630

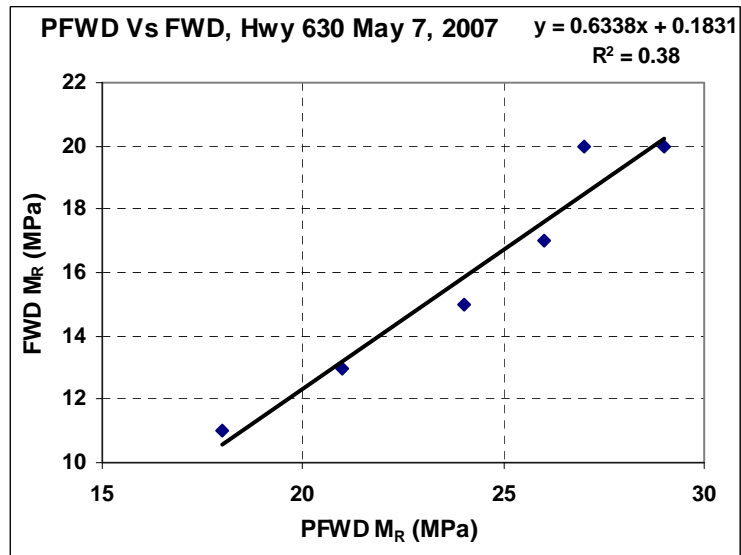


Figure 3.3: PFWD versus FWD, Subgrade Resilient Modulus-Highway 630

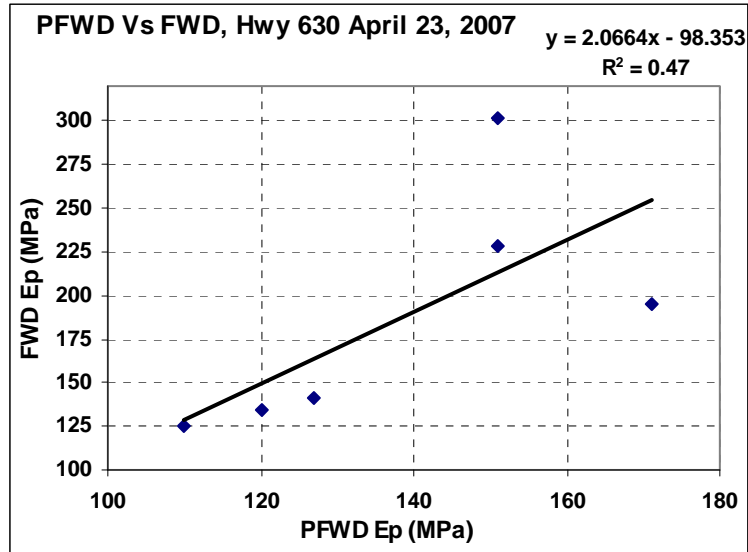


Figure 3.4: PFWD versus FWD, Layer Composite Modulus-Highway 630

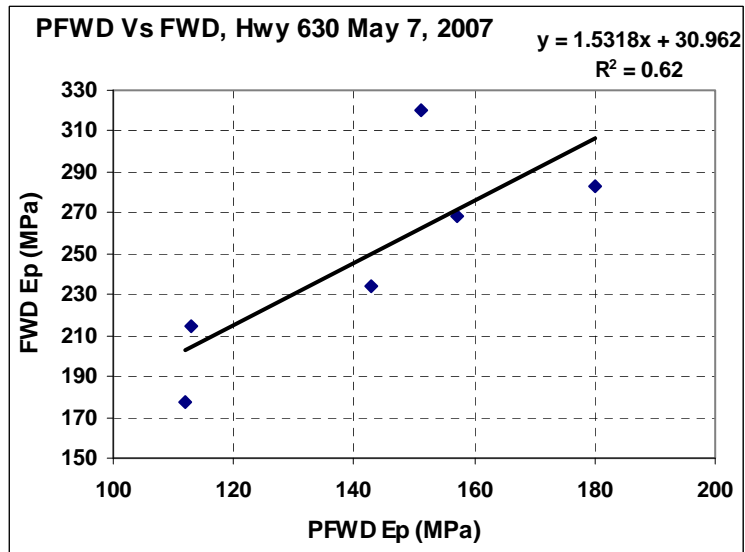


Figure 3.5: PFWD versus FWD, Layer Composite Modulus-Highway 630

Table 3.4 summarizes the deflection recorded by the PFWD and FWD on Highway 630 on the two dates. Figure 3.6 and Figure 3.7 shows the correlation trend and R-squared values when using deflection as the basis for comparison. The correlation gives a R-squared value of 0.62 and 0.81 on April 23, 2007 and May 7, 2007 respectively. The relation is linear and the regression model developed is averaged to derive Equation 1.

Table 3.4: Averaged PFWD and FWD Deflections on Highway 630

SECTION	4/23/2007		5/7/2007	
	PFWD D0 (um)	FWD D0 (um)	PFWD D0 (um)	FWD D0 (um)
1	369	522	330	550
2	369	714	330	680
3	446	1131	372	773
4	495	1256	454	1018
5	442	1159	386	821
6	313	843	290	658

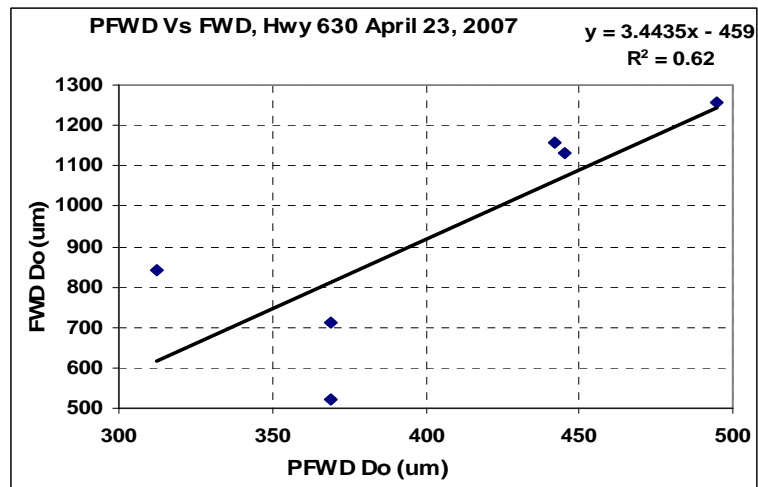


Figure 3.6: FWD versus PFWD for Deflection Do-Hwy 630

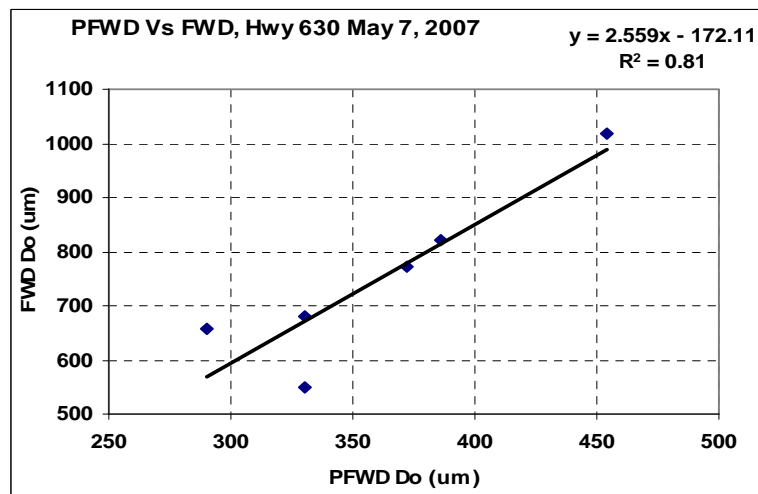


Figure 3.7: FWD versus PFWD for Deflection Do-Hwy 630

3.9 STRUCTURAL EVALUATION OF ONTARIO'S LOW VOLUME ROADS (LVR) IN COMPARISON WITH BRITISH COLUMBIA'S ROADS FOR SLR

At this stage of the study, after correlating the PFWD to the Benkelman Beam, it is inappropriate to adopt BC's CTI threshold deflection values for Ontario's LVRs. The reason for this is that candidate roads in BC for SLR have a different pavement structure. This difference requires evaluating the structural compositions and transforming adequacies in comparable terms. The most basic method of evaluating the structural adequacy of a pavement is the Granular Base Equivalency (GBE) approach [TAC 1997]. Table 3.5 summarizes the structural layer details of roads in BC.

Table 3.5: *Pavement Structure of British Columbia's MOT LVRs based on Unified Soil Classification [TAC 1997]*

Type	Pavement Layer	Thickness (mm)	Subgrade
1	HMA	50	Well Graded Gravel/Sand (GW/SW)
	Aggregate Base Course	150	
2	HMA	50	Grained Soil (GW)
	Aggregate Base Course	300	
3	CMA	25	Grained Soil (GW) or Original surfacing was failed and then was overlain
	Aggregate Base Course	150	
4	CMA	25	Fine Grained inorganic silt and very fine sand (ML)
	Aggregate Base Course	300	

The test sites, which are considered to be representatives of any secondary highway in Ontario typically, have the following structural composition [Table 3.2].

Surface Treatment = 30 mm-70 mm (some surface is overlain during routine maintenance)

Granular Base = 150 mm-300 mm

Subgrade conditions vary from clay, silt and grained soils

In order to compare structural adequacy, it is suggested that the GBE approach be used. A report published by the State of Minnesota Asphalt Pavement Association [Wolters 2003] suggests that 25 mm (1 inch) of Hot Mix Asphalt (HMA) should be considered equal to about 65 mm (2.5 inches) thickness of aggregate base course. Secondly, this report also explains the structural adequacy of the pavement in terms of the tensile strength provided by the asphalt binder present in the HMA mix. Therefore, the roads for SLR in BC differ from the roads in Ontario by two parameters. Firstly BC roads are constructed with

HMA versus Ontario roads are primarily Surface Treated with different thickness. The difference in material result in different tensile strength.

Overall, the HMA pavement structure deflects less under a given load in spring time and has more resistance to vehicular loads even during spring-thaw period. Moreover, this hypothesis can be further extended that higher value of spring deflections will deform the road structure. This justifies the adjustment of threshold PFWD deflection values only for imposition of the ban on full legal axle loads in northern Ontario's Low Volume Roads. The deflection value for lifting the SLR should be kept as is derived in the correlation since these roads recover at a slower pace which is already observed in deflections monitoring during the first round of testing in spring 2008. The strength and the structural adequacy of the roads in BC and northern Ontario differ by approximately 11 % when considering the GBE approach. Thus, the correlated threshold deflection value is reduced to adequately reflect the weaker pavement structure. Thus, 560 μm (0.56 mm) has been used for the imposition of SLR. On the other hand, the threshold for lifting the ban remains at 500 μm (0.5 mm).

3.10 SEASONAL LOAD RESTRICTIONS (SLR) PRACTICE AND DURATION

A flexible road normally transfers traffic loading vertically from one structural layer down to another in such a way that the whole pavement structure deflects bends without rutting or cracking. It can also be interpreted as the loads are uniformly distributed over the structural layers of the flexible pavement. During winter, the pavement structure, mainly in Northern Ontario freezes from the surface to the subgrade layer. Typically frost depth varies from 1.0 metres to as high as 2.0 metres in northern Ontario. The available moisture in the pavement structure upon freezing behaves anomalously and the pavement structure experiences a volumetric expansion called frost heave. Provided this condition remains stable, the road exhibits increased strength that can even justify the allowance of overloaded commercial vehicles. On the other hand, warmer winters and/or the arrival of spring cause temperatures in the soil to oscillate around the freezing point with more or less amplitude and frequency. As a result, the pavement reaches a critical state where the upper layers are thawed while the lower layers remain frozen. This phenomenon is called the freeze-thaw cycle.

Water trapped between the underlying pavement layers saturates the structure and renders it unable to transfer traffic loading properly, and pavement deformation occurs. The deterioration is most dramatic

when the freezing front penetrates into a fine graded, frost susceptible soil, as frost heave is amplified, and the damaging effects of pumping due to partial thawing and saturation are aggravated (*Bullock 2005*). Hence, the most effective and easy action to prevent the pavement from any damage during this freeze – thaw cycle is to impose loads on the axles and is known as the Seasonal Load Restriction (SLR) regulation.

3.10.1 SLR in Ontario

Seasonal load restrictions are imposed each year on low volume routes designated as “Schedule 2 Highways”, usually throughout March, April and May [*MTO 1990*]. Although the SLR periods are commonly called “half load periods”, section 122 of the *Highway Traffic Act* [*Highway Traffic Act 1990*] specifies the load restriction limit to be 5,000 kg per single axle. Vehicles exceeding this limit have to take alternative routes or be subject to the penalties described in the *Act*. Also, oversized load permits, often called Winter Weight Premiums (WWPs), that are usually allowed as long as the pavement structure is frozen and thus assumed to withstand these higher loads, are restricted during an SLR period. SLRs have been typically imposed on or around March 15, usually in response to a three-day warning trend (i.e. a forecast of at least three consecutive days with an average daily temperature above 0⁰ C). The ban is then lifted in response to recommendations by MTO maintenance coordinators who conduct field inspections of the roads to look for signs of strength recovery [*FERIC 2006*]. Indicators include dry road surface cracks, ditches clear of snow and flowing well, and, no residual wetness on the road shoulders after they have been graded. Thus, this makes it an SLR period spanning from eight to ten weeks.

3.10.2 SLR in Canada

A market scan for Transport Canada in 2005 summarized the various methods used in Canada for determining start and stop dates for load restrictions (*Bullock 2005*). The imposition of WWP is most typically done by using fixed dates across Canada, except in Alberta where frost depth and the number of days with temperatures less than 0⁰ Deg C are used. Pavement structures that should receive an SLR schedule are normally identified using design and strength criteria, such as whether or not the frost penetrates down to a frost susceptible subgrade soil. Quantitative methods have progressively been introduced to complement and address limitations of the traditional expert judgment and historical records used in the decision-making process. Calendar-based imposition systems use fixed start dates derived

through analysis of historical thaw data and do not take into consideration annual fluctuations. Used alone, visual observations and engineering judgment often fail to prevent the pavement damage that has been initiated in the lower layers to propagate up to the surface. In an effort to address these concerns, Manitoba, British Columbia, Québec and Alberta have recently adopted more quantitative approaches based on the monitoring of deflection and the use of threshold values (suspected to be associated to strength shifts) to trigger and lift SLR. Other analytical approaches include the use of measured and predicted temperatures as inputs for empirical-mechanistic indicators of the road's strength, such as the thaw index used in Minnesota and in Manitoba. More recently, British Columbia's truckers have shortened SLR periods through the use of Central Tire Inflation (CTI) system to abide by "reduced tire-pressure" periods. The ban period once again falls between eight to ten weeks.

In 2004, the British Columbia (BC) Ministry of Transportation initiated a program to exempt trucks with TPCS from seasonal weight restrictions on approved routes. Forest companies participating in the new BC program have been able to resume hauling with full pay loads two to four weeks sooner at the end of the SLR period. Hence, the new approach in this study, where the repeated use of the PFWD is being introduced as a cost effective tool to monitor the in-situ pavement strength in terms of deflections will enable the agency to announce the real time pavement thaw for SLR imposition and lifting the ban when the pavement starts strength recovery. In addition to this, it will also enable the agency to permit truck equipped with the TPCS technology to carry full pay loads towards the end of the ban period which can potentially result in competitive advantages such as improved harvesting efficiencies, reduced inventories, extended operating seasons and above all, mitigate the anticipated pavement damage.

Figure 3.8 summarizes a schematic flowchart for SLR imposition/lifting and allowing TPCS equipped trucks with full legal loads during the spring-thaw period.

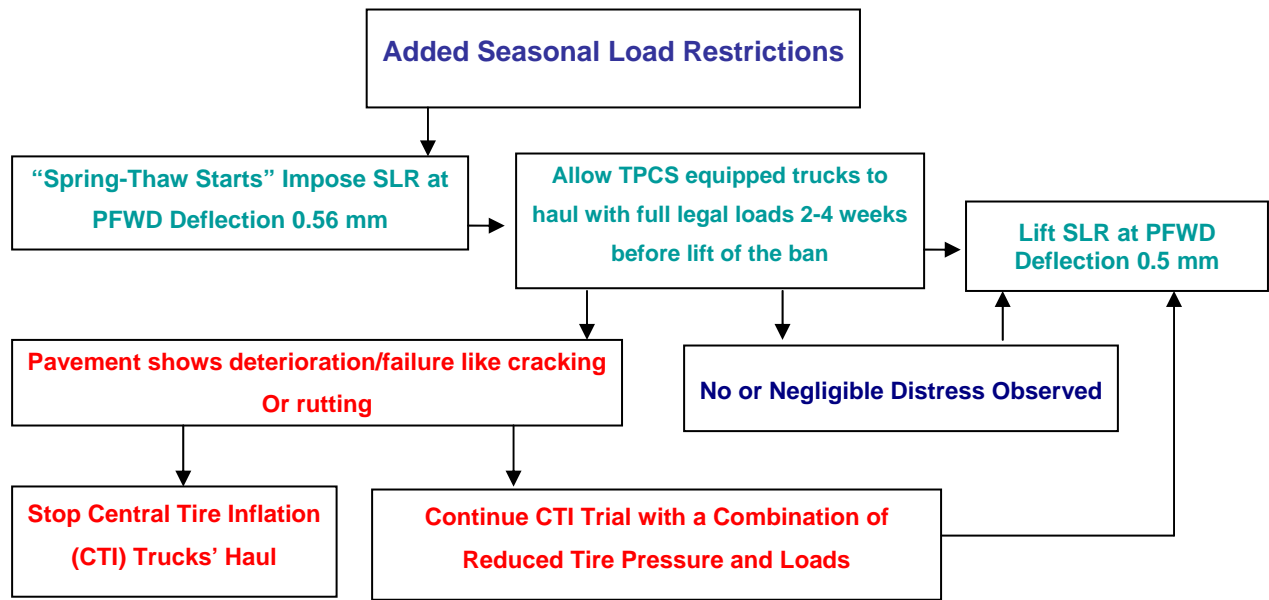


Figure 3.8: Schematic Flow Chart Exhibiting Proposed Methodology for SLR and TPCS Equipped Truck Hauling during CTI Trial Conducted on Highways 601 and 651 During Spring 2008.

3.11 TEST SITES

As mentioned in earlier sections, the preliminary test site was Highway 630 which is a surface treated road located east of North Bay that runs from Highway 17 to the town of Kiosk and was selected by the ministry for the Central Tire Inflation (CTI) pilot project. This road was monitored during the spring of 2007 and the data was used in the preliminary correlations of FWD and PFWD. Later on, by the end of May 2007, two more test routes were identified for the study. These roads are Highway 601 in Dryden-Ontario, starting 1.6 km north of Highway 17, and Highway 651 in Chapleau, Ontario starting at the Highway 101 junction for about 29 km heading north. Location map for test site is provided in Appendix A. Details of test sections and PFWD testing pattern is elaborated in the following sections. The aim is to identify and monitor the freeze-thaw cycles through the repeated use of the PFWD and examine the pavement strength in light of the threshold deflection values. In addition to this, Highway 601 and 651 are instrumented with sensors like a thermistor string to monitor pavement temperature, soil moisture content, relative humidity and air temperature.

3.11.1 Highway 601

Highway 601 is a typical Schedule Two Low Volume surface treated road and is used as an access road to

forestry resources. Table 6 summarizes the repeated PFWD deflection values collected on the highway from September 2007 to June 2008. Here too the deflections are calculated on 95% confidence level, hence are expressed as (Mean+2×Standard Deviation). The length of Highway 601 is 9 kilometers and four test sections are selected with Section 4 fixed as the control section since it was not falling in the haul route of the loaded trucks. Later on, it was found that section four exhibited an extremely weak saturated sub grade therefore it lost its integrity as a control for future deflection monitoring although it was tested and its behavior was monitored regularly. All the test sections were selected as the weakest reaches through visual inspection for pavement distresses like cracks and ruts. It is assumed that the weakest test sections respond promptly to any weather or traffic related changes. These changes can be visibly seen or recorded through changes in the NDT. The ultimate aim is to look for a window where trucks equipped with TPCS can haul full legal loads without increasing pavement damage on these roads during SLR.

Each test section is further divided into twenty test points or locations; each point is 5 meters apart making a 100 meters long test strip. These points are permanently marked on each test section so that testing is performed on the same location on each testing day. All the sections are located on the south bound lane of Highway 601 since the loaded trucks haul from the north. North bound lane of Section 2 is selected as a control for testing after the original control section was relieved from its responsibility as a control. Figure 3.9 shows a typical test section of Highway 601 being tested by the PFWD. Table 3.5 summarizes the deflections surveys done to monitor Highway 601's in-situ strength through repeated PFWD testing.



Figure 3.9: Test Section on Hwy 601, PFWD Testing in Progress

Table 3.6: Highway 601 in-situ strength monitoring through repeated PFWD Testing

Date	Highway 601 - Deflections (um) [Mean + 2×StDev]					
	Sections					
	1	2	3	4 [CS]	(1-3)	(1-4)
25-Sep-07	394	403	370	580	393	484
12-Nov-07	419	341	367	681	385	351
18-Mar-08	218	170	200	262	217	242
24-Mar-08	88	31	98	199	93	142
27-Mar-08	42	13	45	78	56	64
1-Apr-08	190	123	300	270	300	302
4-Apr-08	466	436	484	632	481	554
8-Apr-08	434	397	492	590	467	539
11-Apr-08	492	403	511	697	495	615
15-Apr-08	468	454	557	797	524	699
17-Apr-08	444	479	541	699	517	646
22-Apr-08	469	471	506	833	498	749
29-Apr-08	495	551	575	778	575	677
30-Apr-08	484	550	555	879	550	729
2-May-08	513	528	538	928	540	801
6-May-08	497	482	506	906	506	788
14-May-08	567	466	538	1031	538	861
20-May-08	496	427	500	988	490	811
27-May-08	525	437	519	1074	518	907
3-Jun-08	502	485	503	1014	503	875

Figures 3.10, 3.11, 3.12, and 3.13 show the deflection curves for Section 1, 2, 3, and 4 on Highway 601 respectively. It is observed that the variation in the in-situ pavement strength due to seasonal changes is noted by the PFWD. This validates the use of the PFWD. Moreover, each section has also shown to reach its maximum threshold deflection (Mean + 2×StDev) as the spring-thaw commences in mid April. This confirms the validity of threshold values fixed for imposition of SLR. At the end of the thaw progression, the pavement recovery is seen to be slow and varied; the reason for this is best explained by the fact that the underlying pavement layers are experiencing slow or inefficient drainage.

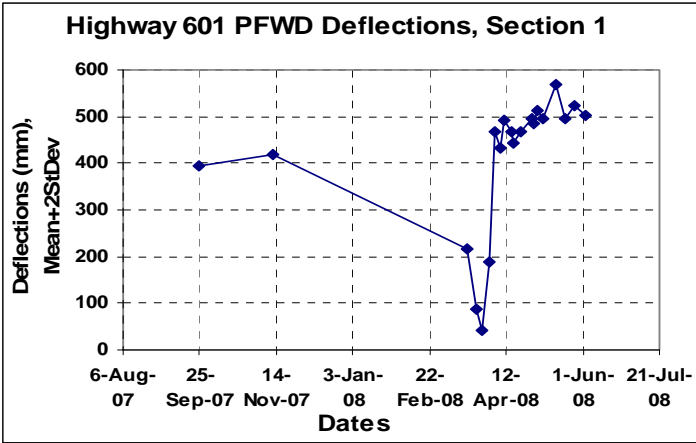


Figure 3.10: Hwy 601, Section 1

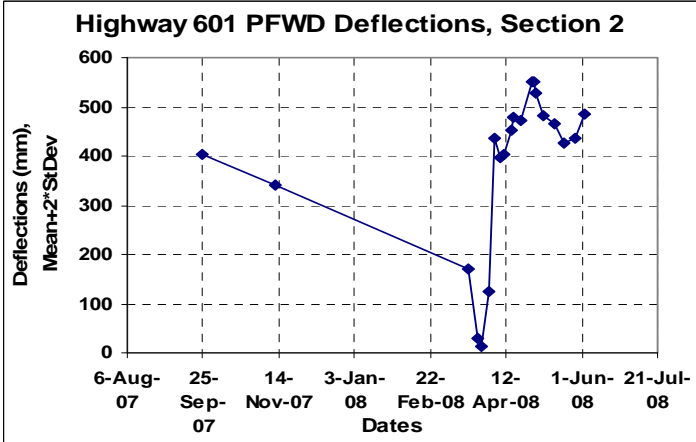


Figure 3.11: Hwy 601, Section 2

Figure 3.16 shows a glimpse of the trend of deflections analyzed all together. It is observed that deflections are following a similar trend for all the sections.

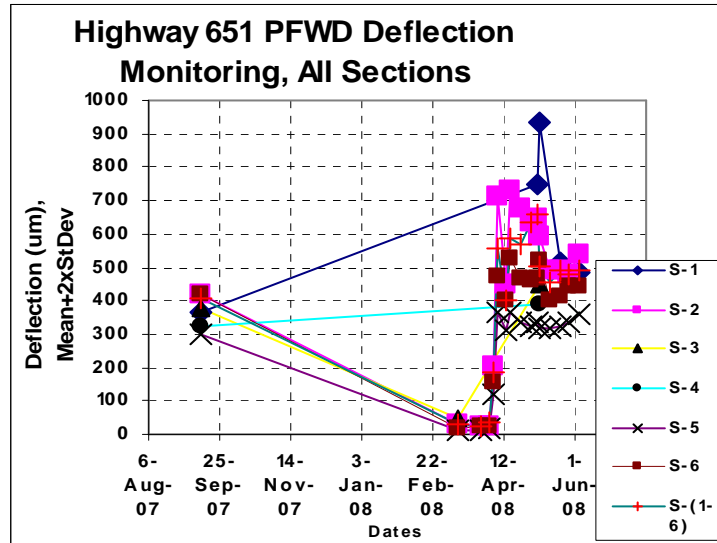


Figure 3.16: Hwy 601, all sections shown.

3.11.2 Highway 651

Highway 651 is also a typical Schedule Two Low Volume surface treated road and is mainly used as an access road to forestry resources only. Table 7 summarizes the repeated PFWD deflection values collected on the highway from September 2007 to June 2008. Here too, the deflections are calculated based on a 95 % confidence level and are expressed as a (Mean+2×Standard Deviation). Highway 651 is located midway between Wawa and Chapleau-Ontario starting at Highway 101 junction for about 29 km north. The length of Highway 651 is about 29 kilometres and seven test sections are selected with Section 6 fixed as the control section since it is not falling in the haul route of the loaded trucks. Like Highway 601, each test section is further divided into twenty test points or locations; each point is 5 meters apart making a 100 meters long test strip at each section. These points are permanently marked on each test section so that testing is performed on the same location on each testing day. Once again, all the sections are located on the south bound lane of the highway since the loaded trucks haul from the north. The north bound lane of Section 2A is selected as an alternate control section for testing to have a ready comparison between the loaded and unloaded lane at a glance. It is observed that both the lanes behave the same.

Table 3.6 summarizes the deflections surveys done to monitor Highway 651's in-situ strength through repeated PFWD testing. It should be noted that Section 1, 3, and 4 are not tested every testing day the reason is explained in the sections ahead. Figure 3.17 shows a typical section of Highway 651 being tested by the PFWD.

Table 3.7: Highway 651 in-situ strength monitoring through repeated PFWD Testing

Date	Highway 651 - Deflections (um) [Mean + 2×StDev]							
	Sections							
	1	2	2A	3	4	5	6 [CS]	Combined Sections
12-Sep-07	365	422	441	377	323	300	420	409
11-Mar-08	x	28	16	45	x	12	20	29
27-Mar-08	x	26	30	x	x	14	25	23
2-Apr-08	x	24	50	x	x	17	25	34
4-Apr-08	x	206	186	x	x	121	157	186
8-Apr-08	x	712	502	x	x	364	474	558
14-Apr-08	x	449	335	x	x	309	402	400
17-Apr-08	x	733	497	x	x	363	526	585
24-Apr-08	x	678	556	x	x	333	467	568
1-May-08	x	632	474	x	x	322	464	632
6-May-08	748	648	543	x	x	336	469	660
7-May-08	933	592	507	451	387	320	522	505
14-May-08	x	493	454	x	x	317	403	455
22-May-08	516	492	427	x	x	325	414	489
28-May-08	x	481	402	x	x	334	441	479
4-Jun-08	485	541	439	x	x	362	444	492



Figure 3.17: Highway 651, Section 6-Control Section

Figure 3.18 shows a tremendous increase in deflection numbers from the survey date till mid April. As indicated in Table 7, Section 1 is tested only on five occasions i.e. with a lesser frequency than the other sections since it had shown extreme weak spots like total top-to-bottom cracks most probably due to insufficient lateral shoulder support and poor drainage. Hence, this section was abandoned and was not tested or analyzed as a representative test section.

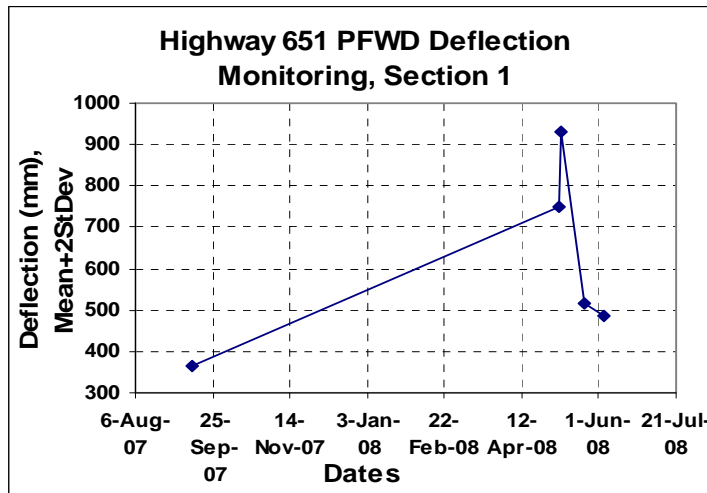


Figure 3.18: Hwy 651, Section 1

Figures 3.19, 3.20, 3.21, and 3.22 shown below indicate the trend of pavement deflections for Sections 2, 2A, 5, and 6 respectively. The deflections follow the same general trend as it did for Highway 601. All these sections experienced thaw in mid April and their strength recovery commences in early or mid May. Highway 651 is known to be stronger structurally and this was further determined through CPATT tests. The geotechnical reports further stated this. The magnitude of the deflection numbers validates the findings of the geotechnical report since Highway 651 has shown considerable resistance to deformation during the freeze-thaw cycle.

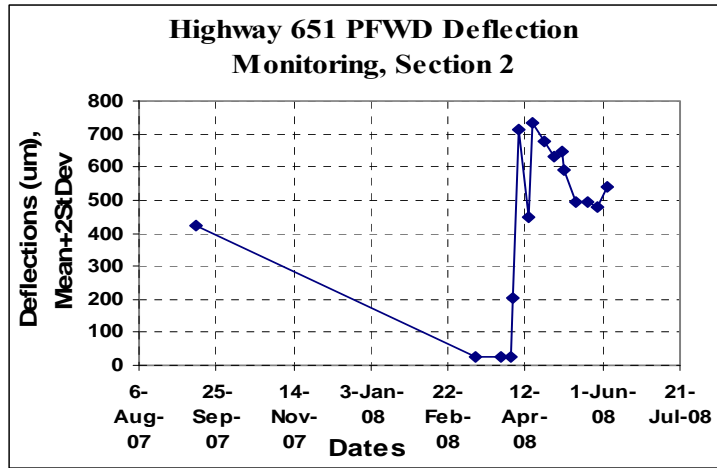


Figure 3.19: Hwy 651, Section 2

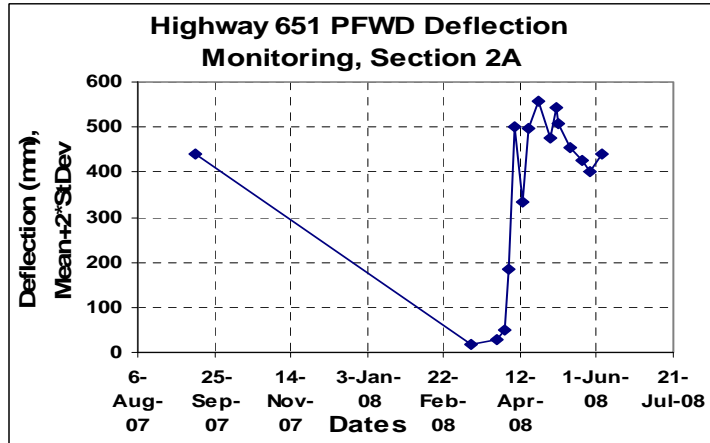


Figure 3.20: Hwy 651, Section 2A

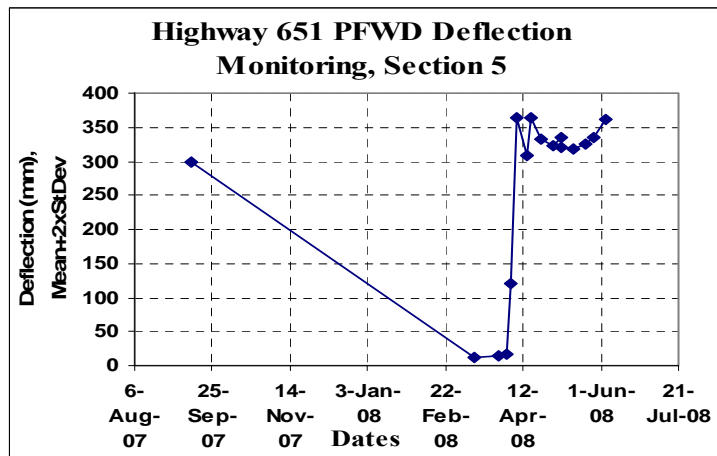


Figure 3.21: Hwy 651, Section 5

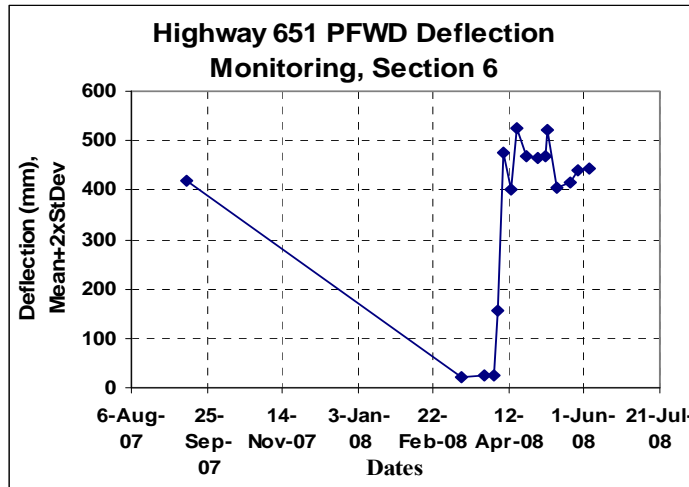


Figure 3.22: Hwy 651, Section 6-Control Section

In Figure 3.23, the deflection values of all the sections are gathered for analysis and their trend is shown. The analysis demonstrates a true representation of the entire highway in terms of PFWD deflections. As already indicated, the Highway has been monitored for deflections since the last fall of 2007 and it is seen that the pavement attains a maximum strength in winter 2008 when the pavement structure is frozen. The deflection data as well as the environmental data indicates that Highway 651 encounters spring-thaw in the second week of April and the pavement starts recovering in the first week of May. Hence, Highway 651 has shown that the SLR period could even be limited to four weeks in case for stronger pavements. But this needs further investigation and monitoring the pavement strength over another period of spring-thaw cycle.

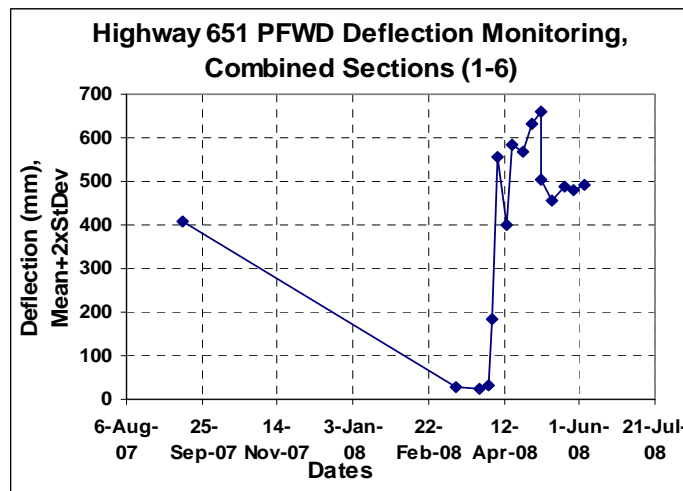


Figure 3.23: Hwy 651, Section 1-6

Figure 3.24 summarizes the general deflection trend of all the sections where each section can readily be compared with the next one. It is observed here that all the sections follow the same trend except for Section 1 which, as already mentioned, is extraordinarily weak.

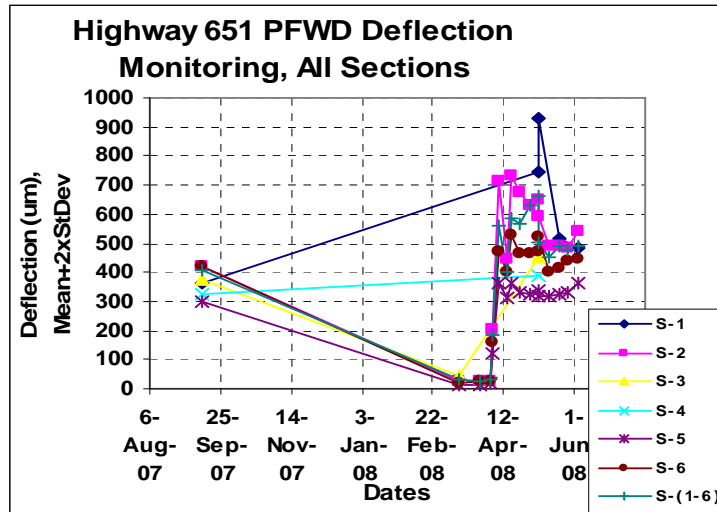


Figure 3.24: Hwy 651, all sections shown

SUMMARY

The PFWD can be used to determine in-situ strength and provides benefits due to its portable nature and also being a less expensive NDT technique. Based on the PFWD rebound values, SLR can be imposed confidently at a spring deflection value of 0.56 mm and lifted when the pavement recovers to a deflection of 0.50 mm.

USE OF INNOVATIVE SENSORS, DATA COLLECTION, AND INTERPRETATION

4.1 INSTRUMENTATION

As noted in the research methodology, the study also involved the design and placement of instrumentation during the fall of 2007 on Hwy 651 and Hwy 601 to monitor the freezing and thawing progression in the pavement structure. This was proposed and executed to further validate the usage of PFWD by conforming the in-situ conditions. To achieve this, the thermistor strings, relative humidity (RH) sensors, air temperature sensors, and water content gauges were installed at the two locations. These monitor in-service pavement real time conditions compared to the surrounding environmental conditions. The use of innovative sensors and data collection techniques are proving to be very informative and are advancing pavement engineering knowledge. The following sections provide installation details including the types of sensors; as well as describe the working principles of the sensors installed at the two locations. It has been observed that the identification of SLR through the use of a PFWD device to monitor in-situ pavement strength has followed the pavement freeze-thaw as expected and was validated by the in-service sensor readings.

4.2 THERMISTOR STRINGS (W0E 404)

The CPATT team worked with Campbell Scientific Inc.'s to purchase the thermistor strings and install them within the pavement structure at various depths as follows: 15 cm, 30 cm, 40 cm, 50 cm, 75 cm, 100 cm, and 150 cm. These heights were selected to best represent in-situ performance.

Figure 4.1 shows one of the thermistor string placed in this research. It has been tied to a wooden stick to enable easier installation and provide support in-service. Figure 4.2, 4.3, and 4.4 show installations on Hwy 601. The thermistor string used in both the sites is a customized single arrangement for temperature sensors meant for recording pavement temperature at the specified depths. The thermistor readings are very important for tracking thaw depth and freezing depth.



Figure 4.1: *View of Thermistor String at Test Site*



Figure 4.2: *Coring for Thermistor Installation.*



Figure 4.3: *Thermistor String Installation Backfilled with the same material, rammed, and sealed with cold mix. (Hwy 651, Nov. 6, 2007)*



Figure 4.4: *The saw cut trench is ready for the string to go in, Hwy 601*

4.3 RELATIVE HUMIDITY AND AIR TEMPERATURE PROBE

The HC-S3 XT Temperature and Relative Humidity Probe was selected as it is a rugged, accurate probe, and are ideal for long-term, unattended applications. The probe uses Hygro Clip technology to measure RH and a Pt100RTD to measure temperature and is suitable for a temperature range of -50 °C to +50 °C. The probe connects directly to Campbell Scientific dataloggers. The CR1000 was selected for this research. Each Hygro Clip probe is 100% interchangeable and can be swapped in

seconds without any loss of accuracy, eliminating the downtime typically required for the recalibration process. A radiation shield (Model 41003-X) is being used since the HC-S3 is exposed to sunlight. When exposed to sunlight, the HC-S3 must be housed in a 41003-X 10-plate radiation shield. The Relative Humidity and Air Temperature probe HC-S3-XT have the following specifications respectively:

Relative Humidity

Operating range: 0 to 100% RH

Accuracy @23°C: ±1.5% RH

Output: 0 - 1 VDC

Typical Long-Term Stability: Better than ±1% RH per year

Temperature

Measurement Range: -40 °C to +60 °C

-50 °C to +50°C (model HC-S3-XT)

Temperature Accuracy: -30°C - +60°C: ±0.2°C

-50°C - +60°C: ±0.6°C (worst case)

Output: 0 - 1 VDC

General

Supply Voltage: 3.5 to 50 VDC (typically powered by data logger's 12 VDC supply)

Current Consumption: < 4 mA

Diameter: 15.25 mm (0.6")

Length: 168 mm (6.6"), and Housing Material: Polycarbonate

4.4 WATER CONTENT REFLECTOMETER

The CS616 Water Content Reflectometer was selected in this research measuring the volumetric water content of porous media, the CS616 uses time domain measurement methods that are sensitive to dielectric permittivity. The probe consists of two 30 cm long stainless steel rods connected to a printed circuit board. The circuit board is encapsulated in epoxy, and is shielded by a four-conductor cable which is connected to the circuit board to supply power, enable probe, and monitor the output. The probe rods can be inserted from the surface or it can be buried at any orientation to the surface. The CS-616 has the following features and is installed on both the sites at subgrade level to monitor the long term water content. It measures the volumetric water content using time-domain reflectometry methods. It is designed for long-term unattended water content monitoring and has an

accuracy $\pm 2.5\%$ VWC (Volumetric Water Content) using standard calibration with a resolution better than 0.1% VWC and measurement time is < 500 microseconds.

Figure 4.5 and 4.6 show the installed Water Content Reflectometer on Highway 651 and 601 respectively.



Figure 4.5: *Installation of CS-616, the probe is inserted into the subgrade, Hwy 651*



Figure 4.6: *The CS-616 probe is inserted horizontally at the subgrade level, Hwy 601*

4.5 DATA LOGGER CR-1000

Both the sites are using CR-1000 data loggers which have the following features:

- 4 MB memory
- Program execution rate of up to 100 Hz
- CS I/O and RS-232 serial ports
- 13-bit analog to digital conversions
- 16-bit H8S Renesas Microcontroller with 32-bit internal CPU architecture
- Temperature compensated real-time clock
- Background system calibration for accurate measurements over time and temperature changes
- Single DAC used for excitation and measurements to give ratio metric measurements
- Gas Discharge Tube (GDT) protected inputs
- Data values stored in tables with a time stamp and record number
- Battery-backed SRAM memory and clock ensuring data, programs, and accurate time are maintained while the CR1000 is disconnected from its main power source
- Measures intelligent serial sensors without using an SDM-SIO4

Figure 4.7 shows a typical CR-1000 data logger installed on both the sites.



Figure 4.7: CR-1000 Datalogger

4.5.1 STORAGE CAPACITY

The CR1000 has 2 MB of FLASH memories for the Operating System, and 4 MB of battery-backed SRAM for CPU usage, program storage, and data storage. Data is stored in a table format. The storage capacity of the CR1000 is increased by using a Compact Flash card.

4.5.2 WIRING PANEL

The CR1000WP is a black, anodized aluminum wiring panel that is compatible with all CR1000 modules. The wiring panel includes switchable 12 V redistributed analog grounds (dispersed among analog channels rather than grouped), a detachable terminal block for 12 V connections, gas-tube spark gaps, and a 12 V supply on pin 8 to power our COM-series modems and other peripherals. The control module easily disconnects from the wiring panel allowing field replacement without rewiring the sensors. A description of the wiring panel's input/output channels follows. Eight differential (16 single-ended) channels measure voltage levels. Resolution on the most sensitive range is 0.67 μ V. The Removable Power Terminal simplifies connection to external power supply.

4.5.3 POWER SUPPLIES

Any 12 V DC source can power the CR1000; a PS100 or BPALK. The PS100 provides a 7 Ahr rechargeable battery that should be connected to a charging source (either a wall charger or solar panel). Solar panels have been provided at both the sites and are used as primary back up of the set up. The BPALK consists of eight non-rechargeable D-cell alkaline batteries with a 7.5 Ahr rating at 20°C. An external AA-cell battery pack supplies power while the D-cells are replaced. Also available are the BP12 and BP24 battery packs, which provide nominal ratings of 12 and 24 Ahrs, respectively. These batteries should be connected to a regulated charging source (e.g., a CH100 connected to an unregulated solar panel or wall charger). The low-power design allows the CR1000 to operate for up to one year on the PS100 power supply, depending on the scan rate, number of sensors, data retrieval method, and external temperature.

The main power source for the data logger on Highway 651 is the PS 100 12 V DC battery backed up by a solar panel. Highway 601 was initially powered by a solar panel, but later on the data logger was provided a live connection from the adjacent hydro source. It is observed that the data loggers on both the sites are working efficiently irrespective of the type of their power sources.

Figure 4.8 and 4.9 illustrates the tripod setting instrument station on Highway 651. Figure 4.10 and 4.11 shows a similar arrangement where the tripod is eliminated and a cabinet is erected for datalogger placement.



Figure 4.8: *Tower mounted with Data logger Cabinet and Solar Panel, Hwy 651*



Figure 4.9: *Sensors installed, Tower Erected, Data logger Programmed and the set up is being tested on Hwy 651*



Figure 4.10: *Erection of Campbell's Tower arrangement eliminated and the mast is being fixed to the Cabinet provided by MTO, Hwy 601*



Figure 4.11: *Sensors installed, connected to data logger and check-run in progress, Hwy 601*

4.6 DATA LOGGER PROGRAM AND DATA ACQUISITION

The data logger CR 1000 is programmed to scan sensor readings after every 5 seconds while the data is stored after an interval of one hour. The data is collected manually from each data logger on a biweekly basis by deputed personnel and sent to the CPATT, University of Waterloo. The data is then

uploaded to the Ministry of Transportation's data portal. The code used to facilitate data downloading is found in Appendix D.

4.7 DATA ACQUISITION

The CR-1000 data logger has a module that measures sensors, drives direct communications and telecommunications, reduces data, controls external devices, and stores data and programs in an on-board, non-volatile storage. The module can simultaneously provide measurement and communication functions. The on-board, BASIC-like programming language supports data processing and analysis routines [Campbell Scientific 2007].

The CR1000 can communicate with a PC using landlines, cellular CDMA, or cellular GPRS/EDGE transceivers. A voice synthesized modem enables anyone to call the CR1000 via phone and receive a verbal report of real-time site conditions. Although this data logger is designed to provide an easy means of data acquisition. Although modem based data download could be achieved, the manual method was agreed upon given there are field staff at both locations and remote nature of the site made it more desirable to have regular checking of the equipment during manual downloads. A CF100 module attached to the CR1000 that can store data on a Compact Flash (CFM 100) card is used to retrieve record data. In addition to this, a PC or a laptop can also be connected to the datalogger via DV3 cable and is able to read the CF card. The data file, after retrieval, can be sent electronically for further analysis or stored in a database. Figure 4.12 shows the VIEW screen where data can be seen and also transported to other destinations.

The screenshot shows a software window titled "C:\Campbellsci\PC400\CR1000-1_Table1.dat". The window contains a data table with the following columns: TIMESTAMP, RECORD, Batt_Vol, Temp_1, Temp_2, Temp_3, Temp_4, Temp_5, Temp_6, Temp_7, AirTC, RH, VM, and PA_uS. The data spans from 05:00:00 on 2008-04-23 to 00:00:00 on 2008-04-25. The RECORD column contains values from 4068 to 4114. The temperature columns (Temp_1 to Temp_7) show values ranging from approximately 7.4 to 13.6. The AirTC column shows values from -2.754 to 1.654. The RH column shows values from 84.3 to 97.2. The VM column shows values from 28 to 31.6. The PA_uS column shows values from 30.03 to 30.12.

TIMESTAMP	RECORD	Batt_Vol	Temp_1	Temp_2	Temp_3	Temp_4	Temp_5	Temp_6	Temp_7	AirTC	RH	VM	PA_uS
"2008-04-23 05:00:00"	4068	12.63	7.474	7.435	6.511	5.13	4.639	1.191	-0.055	4.797	96.9	0.379	30.12
"2008-04-23 06:00:00"	4069	12.62	7.037	7.144	6.357	5.073	4.698	1.231	-0.053	4.508	97.2	0.379	30.12
"2008-04-23 07:00:00"	4070	12.61	6.659	6.863	6.184	5.007	4.747	1.27	-0.052	3.661	95.5	0.379	30.11
"2008-04-23 08:00:00"	4071	12.72	6.334	6.663	6.092	4.992	4.79	1.303	-0.049	4.457	91.9	0.379	30.11
"2008-04-23 09:00:00"	4072	13.57	6.067	6.503	6.019	4.996	4.823	1.336	-0.063	8.54	70.98	0.379	30.11
"2008-04-23 10:00:00"	4073	13.6	6.263	6.244	5.819	4.884	4.846	1.359	-0.069	10.27	51.08	0.379	30.12
"2008-04-23 11:00:00"	4074	13.51	7.446	6.135	5.662	4.786	4.853	1.396	-0.07	11.85	42.38	0.379	30.11
"2008-04-23 12:00:00"	4075	13.44	9.03	6.241	5.546	4.689	4.853	1.406	-0.079	14.4	32.09	0.378	30.1
"2008-04-23 13:00:00"	4076	13.39	10.84	6.58	5.545	4.612	4.852	1.425	-0.089	15.23	31.6	0.378	30.1
"2008-04-23 14:00:00"	4077	13.36	12.59	7.113	5.651	4.593	4.843	1.453	-0.089	16.78	27.11	0.379	30.11
"2008-04-23 15:00:00"	4078	13.34	14.16	7.783	5.86	4.609	4.83	1.469	-0.092	17.06	24.97	0.379	30.11
"2008-04-23 16:00:00"	4079	13.34	15.39	8.5	6.161	4.706	4.821	1.499	-0.091	16.16	25.38	0.379	30.11
"2008-04-23 17:00:00"	4080	13.38	16.19	9.21	6.531	4.833	4.824	1.52	-0.089	14.57	29.12	0.378	30.1
"2008-04-23 18:00:00"	4081	13.41	16.1	9.81	6.91	5.006	4.833	1.539	-0.089	13.54	25.36	0.379	30.11
"2008-04-23 19:00:00"	4082	13.17	15.14	10.16	7.24	5.169	4.862	1.576	-0.071	12.33	28.55	0.379	30.11
"2008-04-23 20:00:00"	4083	12.89	13.94	10.27	7.527	5.356	4.894	1.598	-0.069	9.91	41.6	0.379	30.11
"2008-04-23 21:00:00"	4084	12.78	12.75	10.19	7.712	5.539	4.932	1.617	-0.059	4.054	65.46	0.378	30.1
"2008-04-23 22:00:00"	4085	12.73	11.55	9.97	7.819	5.712	4.998	1.654	-0.052	0.593	75.07	0.378	30.1
"2008-04-23 23:00:00"	4086	12.68	10.43	9.64	7.824	5.812	5.07	1.667	-0.058	-1.106	80.8	0.379	30.11
"2008-04-24 00:00:00"	4087	12.64	9.38	9.23	7.755	5.88	5.147	1.705	-0.058	-1.77	84.3	0.379	30.11
"2008-04-24 01:00:00"	4088	12.61	8.46	8.8	7.602	5.903	5.208	1.728	-0.055	-1.957	86	0.379	30.11
"2008-04-24 02:00:00"	4089	12.58	7.625	8.36	7.43	5.886	5.288	1.749	-0.043	-2.211	87.6	0.378	30.1
"2008-04-24 03:00:00"	4090	12.56	6.885	7.9	7.206	5.819	5.356	1.788	-0.052	-2.415	89.2	0.378	30.1
"2008-04-24 04:00:00"	4091	12.54	6.208	7.452	6.965	5.744	5.406	1.809	-0.051	-2.838	90.7	0.378	30.1
"2008-04-24 05:00:00"	4092	12.53	5.591	7.025	6.705	5.64	5.466	1.849	-0.049	-2.957	91.5	0.378	30.1
"2008-04-24 06:00:00"	4093	12.52	5.033	6.618	6.453	5.515	5.505	1.868	-0.048	-3.127	92.8	0.378	30.1
"2008-04-24 07:00:00"	4094	12.52	4.534	6.221	6.183	5.391	5.545	1.908	-0.038	-2.754	91.2	0.378	30.1
"2008-04-24 08:00:00"	4095	12.71	4.263	5.939	6.007	5.321	5.553	1.945	-0.049	0.059	84	0.378	30.08
"2008-04-24 09:00:00"	4096	13.74	4.254	5.707	5.852	5.263	5.552	1.955	-0.048	8.31	49.62	0.378	30.08
"2008-04-24 10:00:00"	4097	13.66	4.779	5.414	5.569	5.068	5.53	1.972	-0.058	11.32	39.69	0.378	30.08
"2008-04-24 11:00:00"	4098	13.52	6.13	5.32	5.349	4.896	5.503	1.984	-0.065	14.6	33.04	0.377	30.07
"2008-04-24 12:00:00"	4099	13.42	7.972	5.468	5.208	4.747	5.478	1.998	-0.07	17.28	28	0.377	30.07
"2008-04-24 13:00:00"	4100	13.35	10.01	5.889	5.195	4.627	5.435	2.004	-0.083	20.41	22.94	0.377	30.06
"2008-04-24 14:00:00"	4101	13.3	11.91	6.486	5.298	4.577	5.404	2.021	-0.085	21.4	22.01	0.377	30.06
"2008-04-24 15:00:00"	4102	13.28	13.25	7.204	5.52	4.587	5.347	2.031	-0.094	21.07	20.57	0.376	30.04
"2008-04-24 16:00:00"	4103	13.29	13.87	7.917	5.838	4.654	5.308	2.04	-0.085	20.6	20.79	0.377	30.06
"2008-04-24 17:00:00"	4104	13.29	14.29	8.52	6.196	4.779	5.279	2.05	-0.094	20.28	20.96	0.376	30.04
"2008-04-24 18:00:00"	4105	13.3	14.43	9	6.545	4.943	5.261	2.06	-0.093	19.92	23.62	0.376	30.04
"2008-04-24 19:00:00"	4106	13.3	14.08	9.35	6.856	5.098	5.252	2.07	-0.093	18.21	26.25	0.376	30.04
"2008-04-24 20:00:00"	4107	13.01	13.42	9.52	7.094	5.237	5.247	2.075	-0.079	16.5	28.94	0.376	30.04
"2008-04-24 21:00:00"	4108	12.87	12.69	9.58	7.299	5.401	5.266	2.084	-0.079	15.2	28.26	0.376	30.04
"2008-04-24 22:00:00"	4109	12.83	11.94	9.52	7.436	5.546	5.296	2.085	-0.078	13.98	27.73	0.376	30.04
"2008-04-24 23:00:00"	4110	12.81	11.31	9.39	7.518	5.666	5.338	2.098	-0.076	13.43	28.89	0.376	30.03
"2008-04-25 00:00:00"	4111	12.79	10.75	9.21	7.53	5.764	5.388	2.109	-0.074	12.69	30.82	0.376	30.03

Figure 4.12: PC 400 screen demonstrating highway 601 Pavement and Air Data

4.8 FREEZE THAW PHENOMENON AND REAL TIME DATA

It is necessary when considering SLR to identify and understand the freeze thaw cycles. The freeze-thaw areas have been observed to be a function of the precipitation, temperature, soil, and pavement type. In areas where the frost depth penetrates and remains in the subgrade until the spring thaw with relatively few freeze-thaw cycles, is termed as a high freeze area. On the other hand, an area where the frost depth does not penetrate deep into the subgrade and has high number of freeze-thaw cycles is termed as a low freeze area [Huen 2006].

The cyclic freezing and thawing introduces fatigue damage to the pavement structure and can weaken it over prolonged exposure. Capillary forces and lack of drainage through the pavement structure due to top down thawing are factors that contribute to freeze-thaw damage [Tighe 2004, Tighe 2000]. During thaw progression in the pavement structure the vehicle loading is not distributed and transferred as designed. This results in the deformation of the pavement structure. Moreover, in the event of thaw penetrating into

the subgrade, pavement strength conditions become worse, resulting in a need for spring load restrictions in order to mitigate damage. In addition to this, the situation is even worse when the accrued moisture in the pavement structure is not allowed to drain. Lower temperatures during melting ice lenses within the pavement structure make the pavement structure very weak and incapable of carrying full legal loads. Hence, one of the ways to mitigate damage to the pavement structure is to reduce the axle load which is a common practice in the study area. Another possibility to mitigate pavement damage during this pavement unfriendly spring thaw period is to allow full axle loads with reduced tire pressures [Bradley 1997]. The hypothesis behind this possibility is that a greater tire contact area to the pavement results in the distribution of the load over a larger area, reducing the active damage caused by heavy vehicles.

4.9 MITIGATION OF ROAD DAMAGE THROUGH USING TPCS EQUIPPED TRUCKS

TPCS equipped trucks were hauled during the CTI-Trial on Highway 601 and 651 in Spring 2008. The trial was performed towards the end of the SLR period and the pavement was monitored for distresses. The pavement condition survey was evaluated through both visual and Non Destructive Testing PFWD surveys. They demonstrated that the TPCS were road friendly and no damage was observed during and after the trial was over. Detailed analyses are presented in the next chapter.

Threshold PFWD deflection values, already set forth during the preliminary correlations, were the main inputs in the model. The trial was completed with success since the pavement did not exhibit any damage with reduced tire pressures and full axle loads.

The following sections demonstrate the scenarios generated from sensor data in comparison to the instrumented sites and correlating the performance outputs with the in-situ pavement strength as well as SLR.

4.10 FREEZING/THAWING INDICES, FROST DEPTH, AND THAW DURATION

To validate the true SLR duration, the real time pavement and weather data from the data logger is compared with the analytical thaw duration measurement from Equation 4 used in a study conducted by Benjamin in 1999 for the Minnesota Department of Transportation-Cold Weather Road Research facility.

$$D = 0.018(FI) + 25 \quad (4.1)$$

Where FI = Freezing Index, Degree-Days

D = Thaw Duration, Days

The effects from winter temperatures can be estimated by knowing the local Freezing Index (FI) and the Thawing Index (TI). The FI is calculated from the product of the mean daily air temperature below freezing multiplied by the number of days at that temperature. The sum of all these "degree C-days" is the Freezing Index.

The Freezing Index (FI) can also be calculated from Equation 4.2 (*Huenl 2005*) given below:

$$FI = \sum (0^{\circ} \text{C} - T_{\text{MEAN}i}) \quad (4.2)$$

The results from the above equations, datalogger record, and the pavement's in-situ strength during the thaw-weakened period are very similar and conforms the use of either the individual method, combination of two, or all for identification of the SLR.

Table 4.1 and Table 4.2 summarize the FI and TI values calculated from the on-site measured sensor readings. Although both the test sites are located in different areas, both sites have similar cumulative freezing/thawing indices, predicted frost depth and thaw durations. As shown in Table 4.1 and 4.2, the calculated frost depth for Highway 651 differs by 30 mm from the predicted frost depth, and the predicted thaw duration differs by one day only. This calculation indicates that both the highways are behaving in a similar manner despite the fact they are located in different areas of Northern Ontario.

The use of innovative sensors on these access roads to resources has insight into in-service weather impacts. The data will provide the opportunity to relate PFWD measurements to in-situ performance. In addition it will quantify how the freeze thaw cycle impacts strength and performance during SLR.

Table 4.1: Freezing and Thawing Indices on Hwy 601 as worked out from on-site sensor readings.

Month	Freezing			Thawing		
	Mean Air Temperature $T_{\text{mean}}, 0^{\circ} C$	Number of Days Temperature Falling Below $0^{\circ} C$	Freezing Index (FI) [$T_{\text{mean}} \times \text{No. of Days below } 0^{\circ} C$], <i>Deg C-days</i>	Mean Air Temperature $T_{\text{mean}}, 0^{\circ} C$	Number of Days Temperature Falling Above $0^{\circ} C$	Thawing Index (TI) [$T_{\text{mean}} \times \text{No. of Days Above } 0^{\circ} C$], <i>Deg C-days</i>
November	-10.20	15	153.70	-	-	-
December	-14.30	31	443.90	-	-	-
January	-12.90	30	387.10	1.00	1	1.00
February	-13.50	29	392.50	-	-	-
March	-8.50	29	248.10	1.00	2	1.80
April	-2.10	14	29.30	4.20	16	67.60
May	-	-	-	5.40	31	167.20
June	-	-	-	15	30	450
July	-	-	-	20	31	620
August	-	-	-	25	31	775
September	-2	10	20	10	20	200
October	-4	15	60	8	15	220
Σ FI			1735	Σ TI		2333.
Frost Depth FD, $\sqrt{\text{FI}}$ - 42 inches, 106 cm				Thaw Duration D, $0.018 \times \text{FI} + 25$; 56 Days, 08 weeks		

Table 4.2: Freezing and Thawing Indices on Hwy 651 as worked out from on-site sensor readings.

Month	Freezing			Thawing		
	Mean Air Temperature $T_{\text{mean}}, 0^{\circ} C$	Number of Days Temperature Falling Below $0^{\circ} C$	Freezing Index (FI) [$T_{\text{mean}} \times \text{No. of Days below } 0^{\circ} C$], <i>Deg C-days</i>	Mean Air Temperature $T_{\text{mean}}, 0^{\circ} C$	Number of Days Temperature Falling Above $0^{\circ} C$	Thawing Index (TI) [$T_{\text{mean}} \times \text{No. of Days Above } 0^{\circ} C$], <i>Deg C-days</i>
November	-7.30	19	138.70	5.40	5	27.00
December	-11.70	30	350.60	0.70	1	0.70
January	-13.60	27	368.90	1.00	1	1.00
February	-13.80	29	401.80	-	-	-
March	-9.30	30	279.10	2.60	1	2.60
April	-3.30	14	47.00	5.40	16	86.00
May	-	-	-	6.30	31	195.60
June	-	-	-	15	30	450
July	-	-	-	20	31	620
August	-	-	-	25	31	775
September	-2	10	20	10	20	200
October	-4	15	60	8	15	220
Σ FI			1656	Σ TI		2578
Frost Depth FD, $\sqrt{\text{FI}}$ - 41 inches, 103 cm				Thaw Duration D= $0.018 \times \text{FI} + 25$; 55 Days ~08 weeks		

4.11 HISTORICAL DATES FOR SLR IN NORTHERN ONTARIO

As discussed in Section 3.7.4.1, SLRs have been traditionally imposed on or around March 15, usually in response to a three-day warning trend (i.e. a forecast of at least three consecutive days with an average daily temperature above 0⁰ C). The ban is then lifted based on visual field inspections by MTO maintenance coordinators. Table 4.3 summarizes ten years of historical date for impositions and lifting of SLR in Ontario’s north western region. The test sites located on Highway 601 and 651 lie within the locations presented in the table. The historical record indicates that the past SLR period is from eight to ten weeks. Further to this, the thaw-durations for both the regions, as calculated from the sensor readings, equal eight weeks. This is an indication of the critical thaw period. In addition, as described in Sections 3.8.1 and 3.8.2, the pavement starts thawing and loses its strength in the first or the second week of April and starts recovering in mid May. Overall, it would appear that SLR should be delayed from mid March to early April. In any case, it further emphasizes the need to evaluate and monitor in-service predictions.

Table 4.3: *Implementation and Termination Dates for Reduced Loading-Northwestern Region [MTO’s Regional Office Record]*

Year	Thunder Bay (Dryden-Hwy 601 location)			Saulte Ste. Marie (Chapleau-Highway 651 location)		
	Start	End	Duration (weeks)	Start	End	Duration (weeks)
1993	Mar 22	May 20	8	Mar 5	May 17	10
1994	Mar 15	May 24	9	Mar 18	May 24	9
1995	Mar 15	May 23	9	Mar 14	May 12	8
1996	Mar 18	May 27	9	April 1	May 21 & 27	8
1997	Mar 14	May 20	9	Mar 21 & 27	May 26 & June 2	9
1998	Mar 2	May 5	9	Mar 2	May 4	8
1999	Mar 15	May 14	9	Mar 17	May 18	8
2000	Mar 1	May 8 & 13	9-10	Mar 1	May 1 & 8	9
2001	Mar 18-20	May 18-22	9	Mar 18	May 18	8
2002	Mar 19-28	May 21-31	10	Mar 18	May 27	9
2003	Mar 18-20	May 20-23	9	Mar 20	May 20	8

SUMMARY

The Freezing and Thawing Indices calculated from the sensor readings can assist in determining the thaw duration and start and end dates. This analysis, in combination with the deflection data, has shown a possibility delaying or pushing the routine SLR start by two weeks, from March to the second week of April.

Chapter Five

ANALYSING THE EFFECTS OF LOWERED TIRE PRESSURES ON PAVEMENT

5.1 OBJECTIVE

The objective of this study is to determine the effects of operating heavy vehicles at lower tire pressures on roads in severely weakened condition. In order to analyze the effects of lower tire pressures on pavement performance, comparison of the number of load repetitions until failure for each tire load and tire pressure is determined. The failure criteria used in this research was developed by the Asphalt Institute for fatigue cracking and rutting. The formula for fatigue failure defines failure as fatigue cracking in over ten percent of the wheel path area, while rutting failure is defined as 10 mm (0.5 inch) depressions in wheel paths [Grau 1999]. These formulae require determination of two specific strain criteria. For fatigue, horizontal tensile strain at the bottom of the asphalt layer (surface treatment) is determined and the vertical compressive strain at the top of the subgrade is determined for rutting failure. The formulae used are shown below.

Fatigue Failure:

$$\log N_f = 15.947 - 3.291 \log (\epsilon_t/10^{-6}) - 0.854 \log (E/10^3) \quad (5.1)$$

Where N_f = Load repetitions to Failure

ϵ_t = Horizontal Tensile Strain at Bottom of Asphalt Concrete

E = Elastic Modulus of the Asphalt Concrete, (MPa)

Rutting Failure:

$$N_f = 1.077 \times 10^{18} (10^{-6}/\epsilon_v)^{4.4843} \quad (5.2)$$

Where N = Load repetitions to Failure, expressed in numbers

ϵ_v = Vertical Compressive Strain at Top of Subgrade

5.2 CENTRAL TIRE INFLATION (CTI) TRIALS ON HIGHWAY 601 AND 651

After conducting a trial on the initial preliminary test site, Highway 630 in 2006, a second trial was arranged on the other two instrumented sites – Highway 601 and 651. Test loadings were up to legal Gross Commercial Vehicular Weight (GCVW) with no tolerance allowed. The trafficking details are summarized in Table 5.1.

Table 5.1: *Summary of CTI-Trial on Hwy 601 and 651*

Highway	Number of Loads	Avg. GCVW (tones)	Avg. Loads/day	Duration of Trial (weeks)	Hauling Dates
601	383	60.7	16.3	4	April 28-May 24, 2008
651	188	60.5	14.9	3	May 6-May 23, 2008

Truck configurations were all eight axle units. However, they did vary slightly in tire size and configuration, axle loading, and inflation pressure. The TPCS equipped trucks at Highway 601 were all 8-axle trucks with two trailers and had the following configurations:

- Five trucks had a three-axle lead trailer with dual- tires with a single lift axle ahead of a tandem axle group. These trucks all had a rear trailer with a tandem axle group. Their ‘trailer TPCS channel’ controlled all axles as shown in Figure 5.1 and 5.2. Legal weights were 18 t, 23.4 t, and 17.9 t for the drives, lead, and rear trailers, respectively. All tires were 11R22.5 (standard for chip truck) except for two trucks that had 12R22.5 tires on their steering axles.
- One truck was a proper 8-axle Super B-train with a tridem axle group on the lead trailer and a tandem axle group on the rear trailer. Legal weights were 18 t, 22 t, and 17.9 t for the drives, lead, and rear trailers, respectively. All tires were 11R22.5 (standard for a chip truck)

Figure 5.1 and 5.2 shows the Super B-train equipped with the TPCS and hauling over one of the test sections during the trial on Highway 601.



Figure 5.1: Highway 601, Section 3, CTI-Trial with a TPCS equipped chip truck, May 2008



Figure 5.2: Highway 601, Section 3, CTI-Trial with a TPCS equipped chip truck, May 2008

The TPCS- equipped chip trucks that were used on Highway 651 trial were all 8-axle single logging semi-trailers and had the following configurations:

- Five trucks had 5-axle semi-trailers (two lift axles in front of a tridem axle set). The tridem set and rearmost lift axle had dual tire assemblies, which were plumbed together on the same TPCS channel, and thus shared the same TPCS inflation pressures. It was jointly agreed by all the

project participants upon the front lift axle did not need TPCS control if it was equipped with dual tires and was deflated to a constant reduced pressure of 415 kPa (61 psi), and loaded at no more than 6147 kg (13550 lbs, legal single tire loading). This inflation was set in accordance with to Tire and Rim Association recommendations. Tires were 11R24.5 (standard logging truck size) except for the steering axle, tires which were 425/65R22.5 (oversized for better soft ground mobility).

- One truck had a 4-axle semi-trailer (all dual tire assemblies and controlled by a single TPCS channel). This truck also had a pusher axle that could be lifted on the tractor (forward of the drives). Legal load was 4500 kg. The pusher was equipped with non TPCS single tires only but not TPCS. It was deflated to a constant reduced pressure of 50 psi for the trial. This inflation was set according to Tire and Rim Association recommendations. Tires were 11R24.5 (standard logging truck size) except for the steering axle tires which were 425/65R22.5 (oversized for better ground mobility).

Figure 5.3 shows the typical logging truck equipped with the TPCS used in the trial on Highway 651.

Figure 5.4 shows a loaded logging truck during the trial on the same highway.



Figure 5.3: A typical TPCS equipped logging truck on Highway 651



Figure 5.4: A loaded TPCS equipped logging truck on Highway 651, Trial May 2008

5.3 DEVELOPMENT OF DATA AND METHOD OF ANALYSIS

Preliminary input data for the *WESLEA* model is explained in the earlier section. *WESLEA* is a pavement analysis program that can calculate pavement response to applied tire loads. Pavement response is defined in terms of stress, strain, and displacement. The pavement response may then be used to predict the pavement life with respect to fatigue or rutting. The following outline describes the general procedure for using the program.

5.3.1 Fatigue Criteria of Model

Fatigue cracks form as a result of repeated tensile stresses and strains at the bottom of the first pavement layer. The fatigue life may be used in *Miner's Hypothesis* to estimate fatigue damage. An equation developed at the University of Illinois was modified using Mn/ROAD fatigue crack data to predict number of repeated loads until fatigue failure [*Mn/Road 1999*]. The equation is:

$$N_f = 2.83 \times 10^{-6} \left(10^6 / \epsilon_t \right)^{3.148} \quad (5.3)$$

Where:

N_f = number of repeated loads under current structural conditions before a fatigue crack will form.

ϵ_t = maximum horizontal tensile strain at bottom of first layer caused by one pass of current wheel configuration, microstrains.

5.3.2 Rutting Criteria of Model

In *WESLEA*, rutting is attributed to stresses applied to the subgrade. The rutting life may be used in *Miner's Hypothesis* to estimate rutting damage. An equation was developed using Mn/ROAD pavement performance data that predicts rutting of 20 mm (0.5 inch) [*Mn/Road 1999*]

$$N_f = 1.0 \times 10^{16} \left(1/\epsilon_v\right)^{3.87} \quad (5.4)$$

Where:

N_f = number of repeated loads under current structural conditions before rutting failure will occur

ϵ_v = maximum vertical compressive strain at the top of the subgrade caused by one pass of current wheel configuration, microstrain

5.3.3 Miner's Hypothesis to Estimate Pavement Damage

Miner's Hypothesis is used to estimate accumulated pavement damage. As shown below, it is simply the summation of the applied number of loads over the allowable number of loads.

$$D = \sum [n_i / N_{fi}]$$

Where:

D = accumulated damage, ratio

n_i = number of repeated load applications in condition i

N_{fi} = number of allowable repetitions in condition i calculated from fatigue or rutting performance equations.

D is calculated in terms of fatigue and rutting for each set of structural and tire load configuration condition. Failure in a particular mode occurs when $D = 1$. In other words, failure is defined as the number of applied loads exceeding the number of allowable loads.

5.4 INPUTS AND RESULTS FROM WELSEA MODEL SIMULATIONS

As the Welsea model is based on the mechanistic pavement design technique, the input parameters are all set as per site conditions. The available pavement structure thicknesses were available from the borehole data whereas the stiffness values were taken from the PFWD testing done during the trial period. The maximum or the base line tire pressure is 690 kPa (100 psi). The model is developed through considering the pavement as a multilayer structure comprising of surface treatment, granular base, granular subbase, and the existing subgrade soil. Actual material stiffness properties, in terms of layer modulus, are the main inputs in the model with actual layer moduli for site conditions are based on PFWD testing during spring when the pavement is in the weakest condition.

Three set of axles, a single-axle, a tandem-axle, and a tridem-axle, are analyzed and the simulation results are interpreted based on fatigue and rutting criteria as explained in the following sections.

5.4.1 Single-Axle Simulation Model

Table 5.2 summarizes the results from the simulations completed for single-axle truck tire. A total of 80 kN (18 kip) load is applied to the axle and it is observed that for a single-axle arrangement reduction in tire pressure and it has very little effect on the failure criteria. Reduction in tire inflation pressure can only be beneficial with respect to fatigue at tire pressures of 550 kPa (80 psi), 410 kPa (60 psi), and 345 kPa (50 psi) where it has no effect on the rutting of the pavement. The accumulated damage for rutting, at the point where the pavement is extremely weak during the spring-thaw, decreases very gradually by reducing the inflation pressure. The actual simulations are provided in Appendix B.

Table 5.2: Summary of Pavement Failure Results from Single-Axle Simulations

Tire Pressure	690 kPa (100 psi)		550 kPa (80 psi)		410 kPa (60 psi)		345 kPa (50 psi)	
Load Repetitions	<i>Fatigue</i>	<i>Rutting</i>	<i>Fatigue</i>	<i>Rutting</i>	<i>Fatigue</i>	<i>Rutting</i>	<i>Fatigue</i>	<i>Rutting</i>
<i>Applied Truck Passes</i>	100,000	100,000	100,000	100,000	100,000	100,000	100,000	100,000
<i>Passes Allowed by Failure Criteria</i>	78,107	27,538	348,064	28,322	2,209,767	29,746	25,360,598	30,889
<i>Accumulated Damage</i>	1.28	3.68	0.29	3.53	0.02	3.36	0	3.24

5.4.2 Tandem-Axle Simulation Model

The effects of variable tire pressure are simulated and summarized in Table 5.3 for a tandem-axle configuration. It is observed that reduction in tire pressure on a tandem-axle has very little effect on rutting. The fatigue criterion is satisfied when the inflation pressure is reduced to 410 kPa (60 psi).

Table 5.3: Summary of Pavement Failure Results from Tandem-Axle Simulations

Tire Pressure	690 kPa (100 psi)		550 kPa (80 psi)		410 kPa (60 psi)		345 kPa (50 psi)	
Load Repetitions	<i>Fatigue</i>	<i>Rutting</i>	<i>Fatigue</i>	<i>Rutting</i>	<i>Fatigue</i>	<i>Rutting</i>	<i>Fatigue</i>	<i>Rutting</i>
<i>Applied Truck Passes</i>	100,000	100,000	100,000	100,000	100,000	100,000	100,000	100,000
<i>Passes Allowed by Failure Criteria</i>	22,018	427,735	60,338	445,307	268,428	475,898	735,028	492,669
<i>Accumulated Damage</i>	4.54	0.23	1.66	0.22	0.37	0.21	0.14	0.2

5.4.3 Tridem-Axle Simulation Model

Table 5.4 summarizes the results from the simulations completed for tridem-axle truck tires. A total 18 kip (80 kN) load is applied to the tridem-axle and it is observed for this axle arrangement. Reduction in tire pressure has a considerable effect on the failure criteria. It is indeed very interesting that the rutting failure criteria at variable tire pressures remains within a safe range. This is related to the nature of uniform distribution due to the axle configuration. Hence, it can be concluded and would make sense that an increased number of axles will always be friendly to a pavement with regards to rutting. The fatigue failure criteria enter into a safe range when the inflation pressure is dropped to 410 kPa (60 psi). Thus, the simulations concluded that the CTI-Trial be conducted with a tire inflation pressure of 410 kPa (60 psi).

Table 5.4: *Summary of Pavement Failure Results from Tridem-Axle Simulations*

Tire Pressure	690 kPa (100 psi)		550 kPa (80 psi)		410 kPa (60 psi)		345 kPa (50 psi)	
Load Repetitions	Fatigue	Rutting	Fatigue	Rutting	Fatigue	Rutting	Fatigue	Rutting
<i>Applied Truck Passes</i>	100,000	100,000	100,000	100,000	100,000	100,000	100,000	100,000
<i>Passes Allowed by Failure Criteria</i>	16933	1628264	40018	1675772	139810	1757694	318501	1819995
<i>Accumulated Damage</i>	5.91	0.06	2.50	0.06	0.72	0.06	0.31	0.05

The simulation results are annexed in Appendix C.

SUMMARY

Reduced tire pressure has very little effect on rutting or the compressive strains on top of the subgrade soil but plays a very important role in the fatigue cracking due to its effect on the tensile strains at the bottom of the asphalt surface.

CONCLUSIONS AND RECOMMENDATIONS

6.1 STUDY EXPECTATIONS

This study named by the MTO as CTI Phase II, has a number of tasks oriented in many directions. The following major tasks were achieved:

- Evaluating pavement's in-situ strength through NDT testing techniques
- Correlating Falling Weight Deflectometer (FWD) to the Benkelman Beam (BB)
- Introducing a portable and cost effective portable FWD instead of the FWD and BB
- Development of correlations among these NDT instruments
- Exploring the confidence in using the PFWD to monitor pavement strength in terms deflection and stiffness values due to seasonal variations on surface treated roads
- To help agency in identifying true SLR period based on the results of the repeated deflection monitoring of the test sites and real time data from the use of innovative sensors
- Developing threshold PFWD spring deflection values for imposing and lifting SLR
- Evaluate the effect of reduced tire pressure on pavement aiming at looking for a window to allow TPCS equipped trucks to haul with full loads during the last two to three weeks of the SLR period.

6.2 CONCLUSIONS

The conclusions and recommendations reached so far are summarized as follows.

- The PFWD has shown to be a reliable and efficient tool to monitor in-situ pavement strength of surface treated LVR in northern Ontario. The portable nature, inexpensive cost relation to other devices and easy to use make it a good device.
- The use of innovative sensors has provided real time knowledge about weather related parameters

- The in-situ strength monitoring, on both the test sites, indicates that the SLR start date based on the environmental and PFWD data could be delayed by two weeks from March to mid April. Hence, pushing the SLR dates by two weeks will allow the industry to haul with full loads towards the end of the winter and will help the agency to minimize maintenance costs and potential damage, if any, at the end of the thaw period. In short, the SLR will be applied on a more appropriate time.
- The analysis involved using a model whereby the effect of tire pressure is based on actual stiffness values of the different layers of the pavement structure. Failure criteria for fatigue and rutting are taken into account. The number of passes that would actually start damaging the road in fatigue and or rutting is predicted. The axle load is kept constant while the tire pressures are changed from high to low. It is observed from the simulation results that the axle load is the primary factor governing the magnitudes of the horizontal tensile and vertical compressive strains under the surface treatment and above the subgrade respectively. In the event of analyzing the scenario for variable tire pressures, the accumulated damage based on Miner's Failure Criteria, it is observed that reducing the tire pressure on a single-axle configuration is not road friendly at all.
- The tandem and tridem-axle configuration both simulate similar results at a point and it is observed that the accumulated damage due to fatigue and rutting failure enters a safe range when the tire pressure is 410 kPa (60 psi). This condition satisfies Miner's Failure Criteria. Hence, it is concluded that tire pressure plays a significant role in pavement fatigue performance and its effect on compressive strains on top of the subgrade are minimal. The excessive compressive strains that results in rutting of the pavement structure are dominantly controlled by axle loads.

6.2 RECOMMENDATIONS

- The use of the PFWD is therefore recommended to identify proper time for the imposition of SLR on any Schedule 2, LVR in northern Ontario.
- The SLR period can be conservatively shortened to eight weeks based on the results of the two test sites. Further investigation may be required, however, this study showed eight weeks was sufficient.
- The study shows that the SLR start date be delayed by two weeks from March to mid April. This will ensure the roads to have the weight restrictions on the appropriate time and a right balance will be maintained between the pavement strength and the anticipated damage during the spring thaw period.
- The study suggests, based on the simulation results from Miner's Failure Criteria that the use of TPCS is not recommended to be used by trucks with single axle configuration hauling with full axle loads and reduced tire pressures.
- Thus, the study recommends the use of TPCS technology to maintain a maximum reduced tire pressure of 410 kPa (60 psi) for tandem, tridem, and higher number of axle configurations trucks to haul with full axle loads during SLR when the pavement starts recovering from thaw. This period generally falls during the last three to four weeks of the SLR period.

REFERENCES

AASHTO Guide for Design of Pavement Structures, AASHTO Washington D.C. 1993

Bonaquist, R., Surdahi, R., Mogawer, W., “Effect of Tire Pressure on Flexible Pavement Response and Performance.” Transportation Research Record, (1227), TRB, National Research Council, Washington D.C.

Bradley Allan 2006, “Hauling with Full Axle Weights and Reduced Tire Pressures on Weight-Restricted Roads in British Columbia”

Bradley Allan, Mercier Steve, 2006, Forest Engineering Research Institute of Canada, IR-2006-12-22

Bullock, M., “Intelligent Transportation Systems (ITS) for Variable Load Restrictions”, prepared for Transport Canada by IBI Group, March 2005.

Chong, G.J., Wrong, G.A., SP-025- Manual for Condition Rating of Gravel Surface Roads, Research Development Brand, Ontario Ministry of Transportation, August 1989

George, K.P., June 2006, Portable FWD (Prima 100) for In-Situ Sub grade Evaluation, Final Report
Grau R. W., Della-Moretta L.B., “Effects of Variable Tire Pressure on Road surfacing” Transportation Research Record 1291, TRB Washington, DC. 1991.

Kestler, M.A. 2005, “Portable Falling Weight Deflectometers for Tracking Seasonal Stiffness Variations in Asphalt Surfaced Roads”. Department of Civil and Environmental Engineering, University of Maine, USDA Forest Service, New England Transportation Consortium

Kestler, M.A., G. Hanek, M. Truebe, P. Bolander, “Removing Spring Thaw Load Restrictions from Low-Volume Roads”, Transportation Research Record 1652, pp. 188-197, 1999

Kestler, Maureen A. Gordon Hanek, Mark Truebe, and Peter Bolander, “Removing Spring Load Restrictions from Low-Volume Roads, Development of a Cost Effective Method”

Kestler, Maureen A., Thomas Knight, and Audrey S. Krat, June 2000, "Thaw weakening and Load Restriction Practices on Low Volume Road"

Khanna S.K, C.E.G. Justo, IIT University of Roorke, 1999, "Highway Engineering"

Lary J. A Mahoney, J. P. Sharma J., "Evaluation of Frost Related Effects on Pavements", Washington State Transporttaion Center Report, May 1984.

Marshek, K. M., Hudson, W.R., Chenn, H.H., Saraf, C. L. and Connel, R. B. "Effect of Truck Tire Pressure and Axle Load on Pavement Performance" Report No.386-2F, Center for Transportation Research, the University of Texas at Austin, Texas, 1985.

MnRoads, Mechanistic-Empirical Design and MnROAD, "MnROAD Lessons Learned – December 2006", site accessed on July 10, 2008, <http://www.dot.state.mn.us/mnroad/reports/pdfs/medesign.pdf>

Nazzal, M.D.; Abu Farsakh, M.Y.; Alshibli, K.A. and Louay, M.N. (2007) "Evaluating the Light FWD Device for In-situ Measurement of Elastic Modulus of Pavement Layers" Transportation Research Board 2007 Annual Meeting CD-ROM 07-0035.

Nevada Automotive Test Center, Central Tire Inflation", Final Report, U.S. Department of Agriculture, Forest Service, San Dimas equipment Development Center, 1987

Ningyuan, L., Kasmierowski, T., Lane, B., "Long-Term Monitoring of Low-Volume Road Performance in Ontario", Transportation Association of Canada Conference Proceedings, 2006

Notice to Truckers, Spring Load Restrictions 2008, Ministry of Transportation of Ontario, <http://www.mto.gov.on.ca/english/trucks/loadnotice.htm#2/> site accessed April 25, 2008

Oliver, Michael F. Technical Circular T – 11/04, Geotechnical and Pavement Section, Ministry of Transportation, British Columbia, September 2004

Pavement Evaluation Techniques, Washington State DOT, http://training.ce.washington.edu/wsdot/modules/09_pavement_evaluation/09-5_body.htm, site accessed on October 2007.

Reduced Load Periods. Highway Traffic Act, R.S.O. 1990, Chapter H.8, Section 122, http://www.elaws.gov.on.ca/html/statutes/english/elaws_statutes_90h08_e.htm#BK83/, site accessed 04/20/2008.

Richard O. Wolters, P.E., Total Asphalt Versus Granular Base, June 2003, Minnesota Asphalt Pavement Association

Roberts, F.L., Tielking, J.T., Middleton D., Lytton R.L., and Tseng K.H., 1986 “The Effects of Tire Pressures on Flexible Pavements,” Report No. 372-1F, Texas Transportation Institute, College Station Texas

Sebaaly, P., Tabatabaee, N., “Effect of Tire Pressure and Type on Response of Flexible Pavements” Report No. 372-1F, Texas Transportation Institute, College Station Texas, 1986

Sebaaly, P., Tabatabaee, N., 1992 “Effect of Tire Parameters on Pavement Damage and Load Equivalency Factors.” *Journal of Transportation Engineering*, Vol. 118, No. 6

Steinert Bryan C., Dana N. Humphrey, and Maureen A. Kestler August 2005, Portable Falling Weight Deflectometers for Tracking Seasonal Stiffness Variations in Asphalt Surfaced Roads

Steinert, Byran C., Dana N. Humphrey, and Maureen A. Kestler, March , 2005, Portable Falling Weight Deflectometer Study

Stuart, E., Gililand, E., Della-Moretta, L. “The use of Central Tire Inflation Systems on Low-Volume Roads.” *Transportation Research Record 1106*, TRB Washington, D.C. 1987

Taylor, D. J., “National Central Tire Inflation Program-Boise national Forest Field Operational Tests” U.S. Department of Agriculture, Forest Service Equipment Development Center, San Dimas California, 1987

Tighe, S., Huen, K., Mills, B., Perchanok, M., “Development of Tools for Improved Spring Load Restriction Policies in Ontario”, University of Waterloo, Civil Engineering, 2006 Annual Conference of the Transportation Association of Canada, Charlottetown, Prince Edward Island, May 2006.

Tighe, S.L., “Innovation Through Partnership Intelligent Transportation Systems Research and Development for Canada”, Parameter Definition-IBI Group 2004

Tighe, S.L., “Ontario Spring Load Restriction”, Presentation to the Transportation Association of Canada Pavements Standing Committee, Ottawa, 2000.

Tighe, S.L., Joseph Ponniah, “Research Proposal Central Tire Inflation, Phase 11”, May 2007.

Transportation Association of Canada, Pavement Design and Management Guide 1997

US Department of Transportation, National Highway Traffic Safety Administration, “An Evaluation of Existing Tire Pressure Control Systems”, July 2007

Whaley, Andrew M. 1994., “Non-Destructive Testing Equipment: Loadman, Falling Weight Deflectometer, Benkelman Beam, Clegg Hammer, “Department of Civil Engineering, University of Canterbury, Christchurch, New Zealand, 19 pp.

Wore,l Benjamin, P.E., Mn/ROAD Operations, “Improved Spring Load Restriction Guidelines for Minnesota, 1999

The following links are cited for details on the instrumentation used on Hwy 601 and 651:

<http://www.campbellsci.ca/CampbellScientific/Catalogue/CFM100.html>

<http://www.campbellsci.ca/CampbellScientific/Catalogue/CR1000.html>

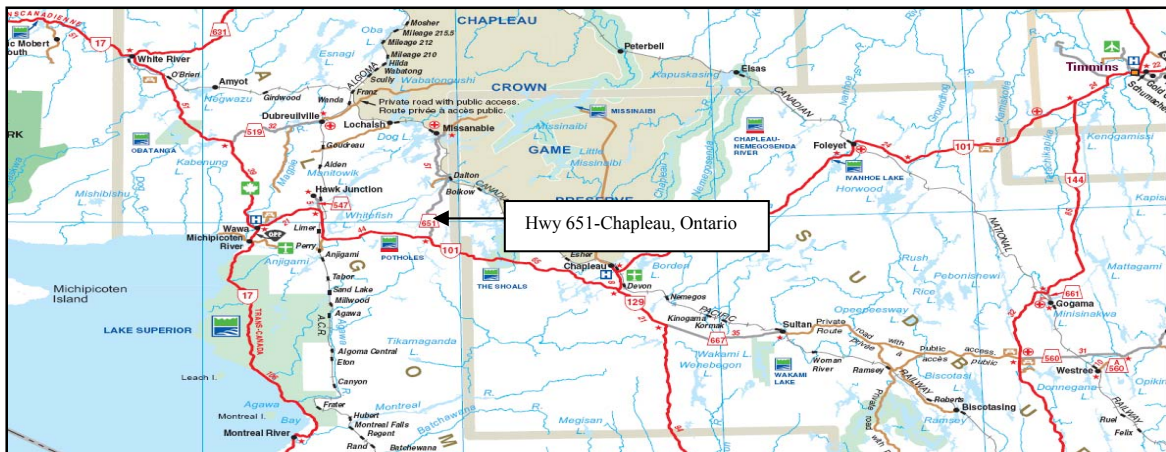
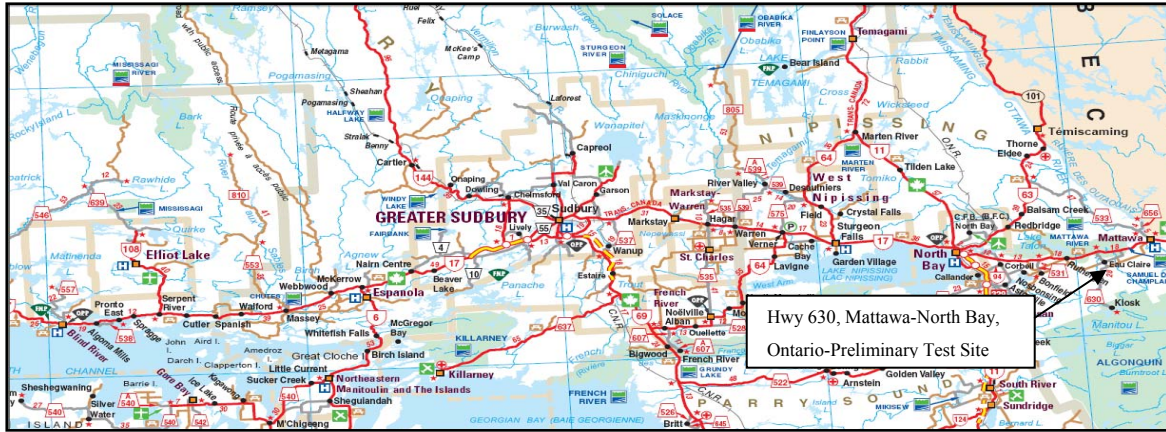
<http://www.campbellsci.ca/CampbellScientific/Catalogue/CS616.html>

<http://www.campbellsci.ca/CampbellScientific/Catalogue/HC-S3.html>

<http://www.campbellsci.ca/CampbellScientific/Catalogue/PC400.html>

<http://www.campbellsci.ca/CampbellScientific/Catalogue/PS100-85.html>

APPENDIX A LOCATION MAPS OF TEST



APPENDIX B

OPERATING PROCEDURES FOR DYNATEST KP100 PORTABLE FWD

**University of
Waterloo**



**Department of
Civil and
Environmental
Engineering**

Phone: 519-888-4567
Fax: 519-888-4300

University of Waterloo
200 University Avenue West
Waterloo, Ontario, Canada
N2L 3G1

www.civil.uwaterloo.ca
www.civil.uwaterloo.ca/CPATT

**Centre for Pavement
and Transportation
Technology**



Measurements should be taken weekly from eight locations at each test site.



Figure 1: load cell

1. Attach load plate to main unit using screws and Allen key. The smallest load plate (200mm diameter)* should be used.



Figure 2 : load plate and load cell

2. Screw in 4 rubber buffers.



Figure 3 : rubber buffers and load cell

3. Screw in bottom shaft to main unit between the rubber buffers. Note that the 2 shafts are NOT interchangeable, so be sure to use the right one.
4. Screw the two extra 5 kg weights onto the main weight using Allen key.

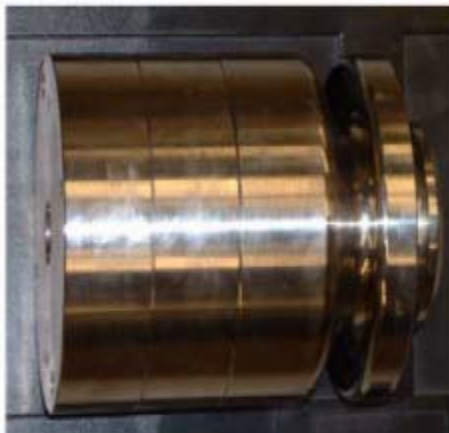


Figure 4 : 20 kg weight

5. Carefully slide the 20 kg weight down the shaft until it rests on the buffers. Note that there is a small grey plastic tube that acts as a guide just inside the weight. This tube should not slide out.

6. Slide trigger handle onto the bottom shaft and tighten.



Figure 5 : trigger handle

7. Screw top shaft onto bottom shaft.
8. Screw handle onto top shaft
9. Move trigger handle to drop height. Do not over tighten the trigger handle. The angle of the handle can be changed by pulling out and rotating to an angle which does not catch the weight.



Figure 6 : assembled PFWD

10. Unscrew knob on Bluetooth battery case.



Figure 7 : Bluetooth signal provider and battery pack

11. Plug in batteries and rescrew battery case. Make sure green light is on; this means that a signal is being sent out to connect with the pocket computer.
12. Turn on pocket computer.
13. Run KP100, located in the start menu.



Figure 8 : Start Menu

14. Enter file name and set file path.

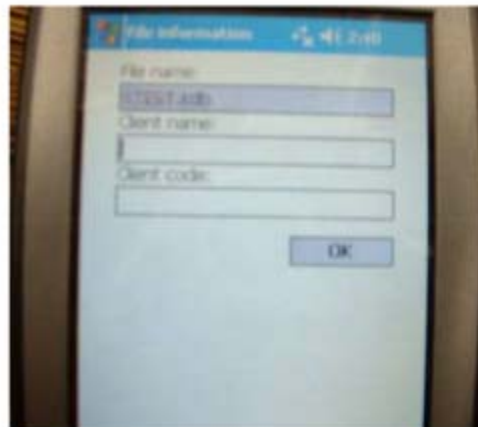
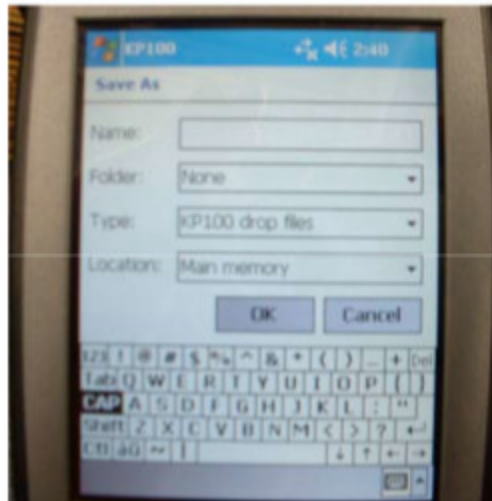


Figure 10 : File Information

15. Record location point, description, temperature and any additional comments.

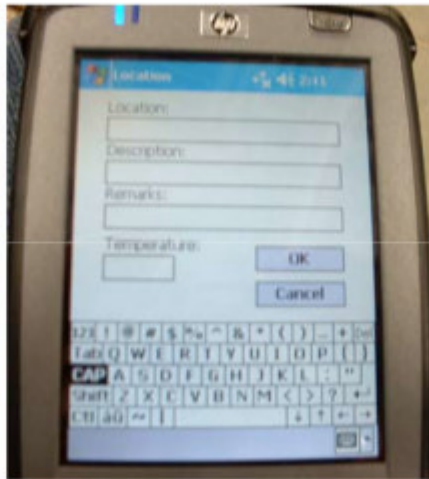


Figure 11 : Location Information

16. In the tools menu click *Connect to Prima*.

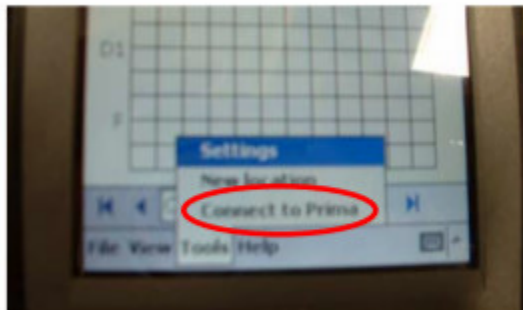


Figure 12 : Tools Menu

17. Click on the Prima icon.

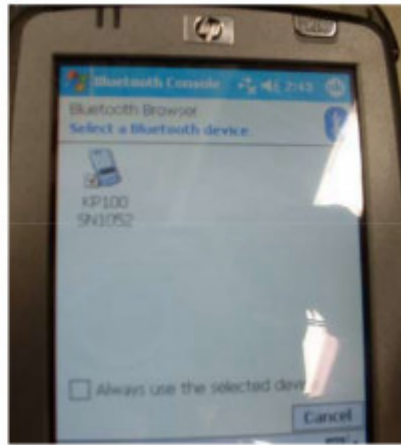


Figure 13 : Bluetooth Connection

18. After the connection is complete, the pocket computer will sound to indicate that it is ready for a drop.

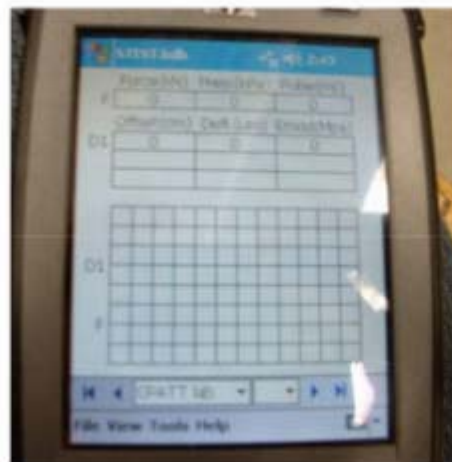
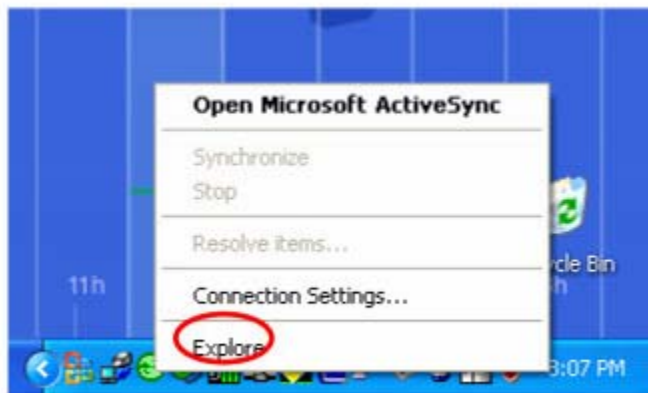
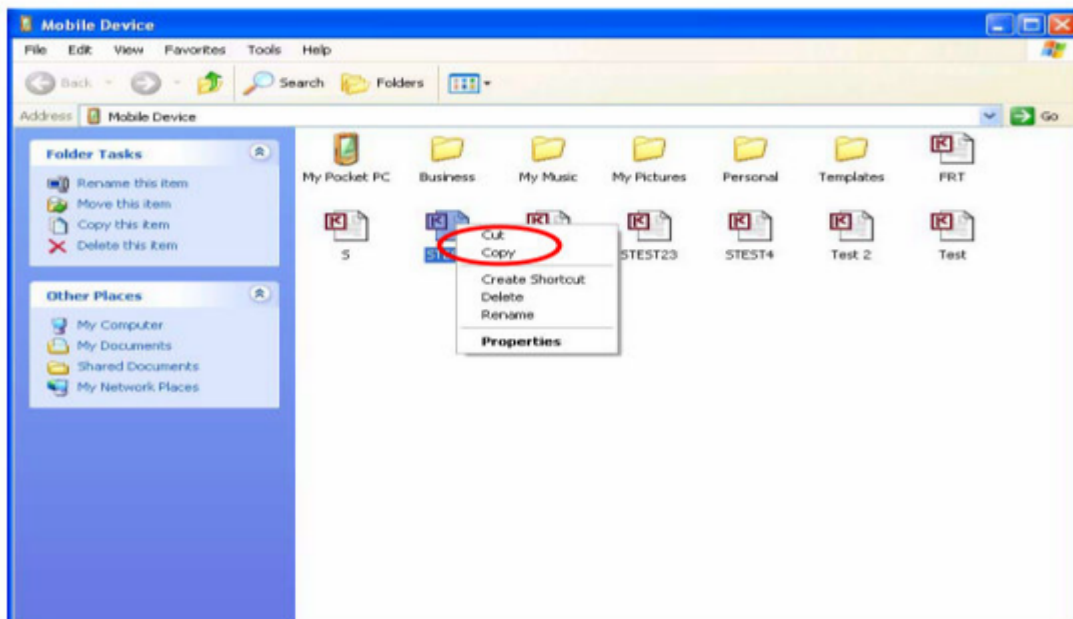


Figure 14 : Test Screen

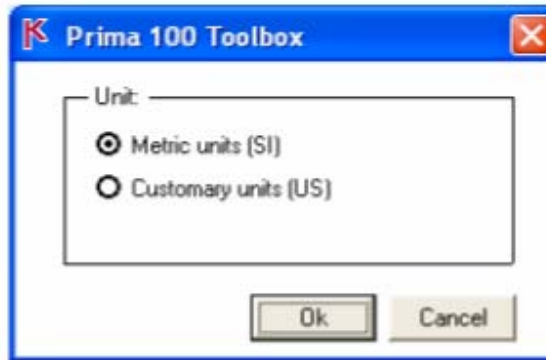
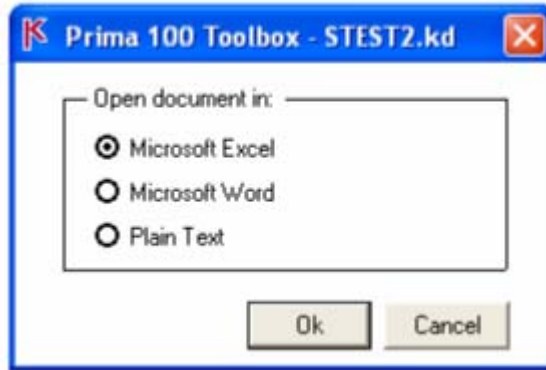
19. Raise the weight and set it below the trigger. Note that when the button on the trigger is up the trigger is locked and the weight will not fall. To release the lock, press the button.
20. Pull the handle and let the weight fall.
21. Repeat steps 19 and 20 for desired number of falls. Six falls at each of three drop heights (850, 630, and 420mm) * are recommended at one location.
22. Once all data has been recorded, connect pocket computer to laptop using cables.
23. Connect the two devices.
24. Left-click the icon on the lower right hand corner of the screen and click explore.



25. Transfer files from pocket computer to laptop using cut and paste.



26. You can open the files on the laptop using Excel if that program is installed on the laptop computer.



* Note: These recommendations taken from:

Steinert, Bryan C., Dana N. Humphrey, and Maureen A. Kestler. "Portable Falling Weight Deflectometer Study." (2005)

APPENDIX C

CR-1000 PROGRAM CODE

The CR-1000 data logger supports its code written in PC 400 software's CR Basic Editor listed below:

'CR1000

'Declare Variables and Units

Public Batt_Volt

Public Temp_1

Public Temp_2

Public Temp_3

Public Temp_4

Public Temp_5

Public Temp_6

Public Temp_7

Public AirTC

Public RH

Public VW

Public PA_uS

Units Batt_Volt=Volts

Units Temp_1=Deg C

Units Temp_2=Deg C

Units Temp_3=Deg C

Units Temp_4=Deg C

Units Temp_5=Deg C

Units Temp_6=Deg C

Units Temp_7=Deg C

Units AirTC=Deg C

Units RH=%

Units PA_uS=uSec

'Define Data Tables

DataTable(Table1,True,-1)

 DataInterval (0, 60, Min, 10)

 CardOut(0,-1)

 Average (1, Batt_Volt, FP2, False)

 Sample (1, Temp_1, FP2)

 Sample (1, Temp_2, FP2)

 Sample (1, Temp_3, FP2)

 Sample (1, Temp_4, FP2)

 Sample (1, Temp_5, FP2)

 Sample (1, Temp_6, FP2)

 Sample (1, Temp_7, FP2)

 Sample (1, AirTC, FP2)

 Sample (1, RH, FP2)

 Sample (1, VW, FP2)

 Sample (1, PA_uS, FP2)

End Table

DataTable (Table2, True,-1)

 DataInterval (0, 60, Min, 10)

 Minimum (1, Batt_Volt, FP2, False, False)

EndTable

'Main Program

BeginProg

 Scan (1, Min, 1, 0)

 'Default Datalogger Battery Voltage measurement Batt_Volt:

 Battery (Batt_Volt)

 '107 Temperature Probe measurement Temp_1:

 Therm107 (Temp_1, 1, 1, 1, 0, _60Hz, 1.0, 0.0)

 '107 Temperature Probe measurement Temp_2:

 Therm107 (Temp_2, 1, 2, 1, 0, _60Hz, 1.0, 0.0)

 '107 Temperature Probe measurement Temp_3:

 Therm107 (Temp_3, 1, 3, 1, 0, _60Hz, 1.0, 0.0)

```
'107 Temperature Probe measurement Temp_4:
Therm107 (Temp_4, 1, 4, 1, 0, _60Hz, 1.0, 0.0)
'107 Temperature Probe measurement Temp_5:
Therm107 (Temp_5, 1, 5, 2, 0, _60Hz, 1.0, 0.0)
'107 Temperature Probe measurement Temp_6:
Therm107 (Temp_6, 1, 6, 2, 0, _60Hz, 1.0, 0.0)
'107 Temperature Probe measurement Temp_7:
Therm107 (Temp_7, 1, 7, 2, 0, _60Hz, 1.0, 0.0)
'HC-3-xt Temperature and Relative Humidity
VoltDiff (AirTC, 1, mV2500, 5, True, 0, _60Hz, 0.1,-50)
VoltDiff (RH, 1, mV2500, 6, True, 0, _60Hz, 0.1, 0)
```

```
'CS616 Water Content Reflectometer measurements VW and PA_uS:
If If Time (0, 1, Hr) Then
    CS616 (PA_uS, 1, 8, 2, 1, 1, 0)
    VW=-0.0663+ (-0.0063*PA_uS) + (0.0007*PA_uS^2)
EndIf
'Call Data Tables and Store Data
CallTable (Table1)
CallTable (Table2)
```

```
NextScan
EndProg
```

APPENDIX D

WESLEA for Windows - Simulation Output

Axle Type: Tridem

Tire Pressure: 690 kPa

Date: Mon Jul 14 01:26:44
2008

STRUCTURAL INFORMATION

Layer	Modulus (MPa)	Poisson	Height (cm)	Slip
1	551.6	0.35	3	1
2	137.9	0.35	13	1
3	137.9	0.35	17	1
4	82.7	0.35	2537	1
5	82.7	0.35	Infinite	

LOADING CONFIGURATION

Tire#	X (cm)	Y (cm)	Load (kN)	Pressure (kPa)
1	0	0	7	690
2	34.29	0	7	690
3	34.29	137.16	7	690
4	0	137.16	7	690
5	0	274.3	7	690
6	34.29	274.3	7	690

PREDICTED PAVEMENT LIFE

	690 kPa	
	FATIGUE	RUTTING
Applied	100000	100000
Allowed	16933	2E+06
Damage	5.91	0.06

ENGINEERING RESPONSES

Loc#	Layer	Coordinates (cm)			Normal Stress (kPa)			Normal MicroStrain			Displacement (micrometer)			Shear Stress (kPa)		
		X	Y	Z	X	Y	Z	X	Y	Z	X	Y	Z	YZ	XZ	XY
1	1	0	0	3	-379	-378.5	531.1	-783.85	-782.79	1443.5	-6.21	-8.58	514.09	0	-1.73	-0.4
2	1	17.15	0	3	132.2	43.99	1.22	210.92	-4.89	-109.56	0	-8.66	279.84	0	0	0
3	1	17.15	68.58	3	13.31	-3.42	0.05	26.28	-14.69	-6.19	0	-3.92	158.88	0	0	0
4	1	0	68.58	3	12.14	-2.96	0.04	23.85	-13.1	-5.74	-4.36	-3.9	155.57	0	-0.15	-0.11
5	1	17.15	137.2	3	133.4	42.97	1.22	213.76	-7.5	-109.68	0	0	297	0	0	0
6	4	0	0	32.99	1.85	-1.44	28.12	-90.47	-144.33	338.28	13.46	0.15	222.87	-0.28	-4.5	0.05
7	4	17.15	0	32.99	3.89	-1.57	27.89	-64.31	-153.61	327.49	0	0.22	231.8	-0.29	0	0
8	4	17.15	68.58	32.99	0.73	5.8	2.65	-26.87	55.75	4.43	0	-0.7	161.05	-0.06	0	0
9	4	0	68.58	32.99	0.89	5.39	2.47	-22.53	50.96	3.27	4.36	-0.71	157.72	-0.06	-0.76	0.01
10	4	17.15	137.2	32.99	3.98	-1.05	27.96	-65.73	-147.94	325.71	0	0	249.31	0	0	0

WESLEA for Windows - Simulation Output

Axle Type: Tridem
Tire Pressure: 540 kPa

Date: Mon Jul 14 01:26:44
2008

STRUCTURAL INFORMATION

Layer	Modulus	Poisson	Height	Slip
	(MPa)		(cm)	
1	551.6	0.35	3	1
2	137.9	0.35	13	1
3	137.9	0.35	16.99	1
4	82.7	0.35	2537	1
5	82.7	0.35	Infinite	

LOADING CONFIGURATION

Tire#	X	Y	Load	Pressure
	(cm)	(cm)	(kN)	(kPa)
1	0	0	7	550
2	34.29	0	7	550
3	34.29	137.16	7	550
4	0	137.16	7	550
5	0	274.32	7	550
6	34.29	274.32	7	550

PREDICTED PAVEMENT LIFE

	550 kPa	
	FATIGUE	RUTTING
Applied	100000	100000
Allowed	40018	2E+06
Damage	2.5	0.06

ENGINEERING RESPONSES

Loc#	Layer	Coordinates (cm)			Normal Stress (kPa)			Normal MicroStrain			Displacement (micrometer)			Shear Stress (kPa)		
		X	Y	Z	X	Y	Z	X	Y	Z	X	Y	Z	YZ	XZ	XY
1	1	0	0	3	-262.9	-262.6	451.4	-596.46	-595.57	1151.7	-6.2	-8.58	489.89	0	-1.73	-0.4
2	1	17.15	0	3	135.3	44.34	1.73	216.13	-6.6	-110.87	0	-8.66	280.58	0	0	0
3	1	17.15	68.58	3	13.32	-3.39	0.05	26.28	-14.64	-6.21	0	-3.92	158.9	0	0	0
4	1	0	68.58	3	12.14	-2.93	0.04	23.85	-13.06	-5.76	-4.36	-3.9	155.59	0	-0.15	-0.11
5	1	17.15	137.2	3	136.6	43.32	1.73	218.97	-9.21	-110.99	0	0	297.74	0	0	0
6	4	0	0	32.99	1.89	-1.39	27.94	-89.55	-143.08	335.77	13.44	0.15	222.56	-0.28	-4.49	0.05
7	4	17.15	0	32.99	3.84	-1.52	27.84	-64.84	-152.57	326.78	0	0.22	231.57	-0.29	0	0
8	4	17.15	68.58	32.99	0.74	5.8	2.66	-26.88	55.72	4.49	0	-0.7	161.07	-0.06	0	0
9	4	0	68.58	32.99	0.89	5.39	2.47	-22.53	50.94	3.32	4.36	-0.71	157.74	-0.06	-0.77	0.01
10	4	17.15	137.2	32.99	3.93	-1	27.9	-66.26	-146.9	325	0	0	249.08	0	0	0

WESLEA for Windows - Simulation Output

Axle Type: Tridem
Tire Pressure: 345 kPa

Date: Mon Jul 14 01:31:28
2008

STRUCTURAL INFORMATION

Layer	Modulus (MPa)	Poisson	Height (cm)	Slip
1	551.6	0.35	3	1
2	137.9	0.35	13	1
3	137.9	0.35	16.99	1
4	82.7	0.35	2537	1
5	82.7	0.35	Infinite	

LOADING CONFIGURATION

Tire#	X (cm)	Y (cm)	Load (kN)	Pressure (kPa)
1	0	0	7	345
2	34.29	0	7	345
3	34.29	137.16	7	345
4	0	137.16	7	345
5	0	274.32	7	345
6	34.29	274.32	7	345

PREDICTED PAVEMENT LIFE

	550 kPa	
	FATIGUE	RUTTING
Applied	100000	100000
Allowed	318501	2E+06
Damage	0.31	0.05

ENGINEERING RESPONSES

Loc#	Layer	Coordinates (cm)			Normal Stress (kPa)			Normal MicroStrain			Displacement (micrometer)			Shear Stress (kPa)		
		X	Y	Z	X	Y	Z	X	Y	Z	X	Y	Z	YZ	XZ	XY
1	1	0	0	3	-93.23	-93.06	313.1	-308.61	-308.21	685.76	-6.16	-8.57	440.22	0	-1.75	-0.4
2	1	17.15	0	3	144.4	45.34	3.59	230.71	-11.7	-113.87	0	-8.66	282.85	0	0	0
3	1	17.15	68.58	3	13.35	-3.31	0.05	26.27	-14.51	-6.27	0	-3.92	158.96	0	0	0
4	1	0	68.58	3	12.17	-2.86	0.05	23.84	-12.95	-5.82	-4.36	-3.9	155.65	0	-0.15	-0.11
5	1	17.15	137.2	3	145.6	44.32	3.59	233.55	-14.31	-114	0	0	300.02	0	0	0
6	4	0	0	32.99	1.98	-1.24	27.44	-86.96	-139.52	328.68	13.36	0.16	221.66	-0.28	-4.48	0.05
7	4	17.15	0	32.99	3.71	-1.39	27.66	-66.29	-149.59	324.65	0	0.22	230.9	-0.29	0	0
8	4	17.15	68.58	32.99	0.74	5.8	2.67	-26.89	55.64	4.65	0	-0.7	161.13	-0.06	0	0
9	4	0	68.58	32.99	0.89	5.39	2.48	-22.54	50.86	3.47	4.36	-0.71	157.8	-0.06	-0.77	0.01
10	4	17.15	137.2	32.99	3.8	-0.86	27.73	-67.71	-143.92	322.86	0	0	248.42	0	0	0

WESLEA for Windows - Simulation Output

Axle Type: **Tandem**

Tire Pressure: **690 kPa**

Date: Mon Jul 14 03:07:18
2008

STRUCTURAL INFORMATION

Layer	Modulus (MPa)	Poisson	Height (cm)	Slip
1	551.6	0.35	3	1
2	137.9	0.35	13	1
3	137.9	0.35	16.99	1
4	82.7	0.35	2537	1
5	82.7	0.35	Infinite	

LOADING CONFIGURATION

Tire#	X (cm)	Y (cm)	Load (kN)	Pressure (kPa)
1	0	0	7	550
2	0	0	10	690
3	34.29	0	10	690
4	34.29	137.16	10	690
5	0	137.16	10	690
6	34.29	274.32	7	550

***PREDICTED PAVEMENT

	690 kPa	
	FATIGUE	RUTTING
Applied	100000	100000
Allowed	22018	427735
Damage	4.54	0.23

ENGINEERING RESPONSES

Loc#	Layer	Coordinates (cm)			Normal Stress (kPa)			Normal MicroStrain			Displacement (micrometer)			Shear Stress (kPa)		
		X	Y	Z	X	Y	Z	X	Y	Z	X	Y	Z	YZ	XZ	XY
1	1	0	0	3	-296.2	-294.5	584.8	-721.11	-717.1	1435	-8.57	-7.87	655.52	0	-2.48	-0.51
2	1	17.15	0	3	195.7	64.17	3.02	312.18	-9.76	-159.43	0	-7.97	377.05	0	0	0
3	1	17.15	68.58	3	17.86	-3.94	0.07	34.84	-18.53	-8.7	0	0	194.37	0	0	0
4	1	0	68.58	3	16.19	-3.32	0.06	31.43	-16.34	-8.05	-5.78	0	189.76	0	-0.22	0
5	4	0	0	32.99	2.64	-2.01	39.74	-127.7	-203.68	477.84	19.28	2.01	293.06	-0.37	-6.41	0.07
6	4	17.15	0	32.99	5.37	-2.21	39.7	-93.78	-217.46	466.71	0	2.11	305.96	-0.38	0	0
7	4	17.15	68.58	32.99	0.93	8.06	3.79	-38.9	77.51	7.75	0	0	197.24	0	0	0
8	4	0	68.58	32.99	1.15	7.48	3.52	-32.71	70.72	6.07	6.31	0	192.6	0	-1.09	0

WESLEA for Windows - Simulation Output

Axle Type: Tandem

Tire Pressure: 410 kPa

Date: Mon Jul 14 03:09:17
2008

STRUCTURAL INFORMATION

Layer	Modulus	Poisson	Height	Slip
	(MPa)		(cm)	
1	551.6	0.35	3	1
2	137.9	0.35	13	1
3	137.9	0.35	16.99	1
4	82.7	0.35	2537	1
5	82.7	0.35	Infinite	

LOADING CONFIGURATION

Tire#	X	Y	Load	Pressure
	(cm)	(cm)		
1	0	0	10	410
2	34.29	0	10	410
3	34.29	137.16	10	410
4	0	137.16	10	410

***PREDICTED PAVEMENT

	410 kPa	
	FATIGUE	RUTTING
Applied	100000	100000
Allowed	268428	475898
Damage	0.37	0.21

ENGINEERING RESPONSES

Loc#	Layer	Coordinates (cm)			Normal Stress (kPa)			Normal MicroStrain			Displacement (micrometer)			Shear Stress (kPa)		
		X	Y	Z	X	Y	Z	X	Y	Z	X	Y	Z	YZ	XZ	XY
1	1	0	0	3	-69.74	-68.46	382.7	-325.84	-322.72	781.55	-8.51	-7.87	577.05	0	-2.51	-0.51
2	1	17.15	0	3	212.2	66.03	6.94	338.38	-19.34	-163.95	0	-7.97	381.41	0	0	0
3	1	17.15	68.58	3	17.9	-3.79	0.07	34.82	-18.29	-8.82	0	0	194.49	0	0	0
4	1	0	68.58	3	16.23	-3.19	0.07	31.41	-16.13	-8.15	-5.77	0	189.87	0	-0.22	0
5	1	0	0	32.99	2.81	-1.73	38.82	-122.98	-197.14	464.85	19.13	2.02	291.4	-0.37	-6.38	0.07
6	4	17.15	0	32.99	5.13	-1.95	39.37	-96.39	-211.93	462.65	0	2.11	304.71	-0.38	0	0
7	4	17.15	68.58	32.99	0.94	8.06	3.82	-38.92	77.35	8.06	0	0	197.35	0	0	0
8	4	0	68.58	32.99	1.15	7.48	3.55	-32.73	70.58	6.35	6.31	0	192.71	0	-1.09	0

WESLEA for Windows - Simulation Output

Axle Type: Tandem

Tire Pressure: 345 kPa

Date: Mon Jul 14 03:10:17
2008

STRUCTURAL INFORMATION

Layer	Modulus (MPa)	Poisson	Height (cm)	Slip
1	551.6	0.35	3	1
2	137.9	0.35	13	1
3	137.9	0.35	16.99	1
4	82.7	0.35	2537	1
5	82.7	0.35	Infinite	

LOADING CONFIGURATION

Tire#	X (cm)	Y (cm)	Load (kN)	Pressure (kPa)
1	0	0	10	345
2	34.29	0	10	345
3	34.29	137.16	10	345
4	0	137.16	10	345

***PREDICTED PAVEMENT

	345 kPa	
	FATIGUE	RUTTING
Applied	100000	100000
Allowed	735028	492669
Damage	0.14	0.2

ENGINEERING RESPONSES

Loc#	Layer	Coordinates (cm)			Normal Stress (kPa)			Normal MicroStrain			Displacement (micrometer)			Shear Stress (kPa)		
		X	Y	Z	X	Y	Z	X	Y	Z	X	Y	Z	YZ	XZ	XY
1	1	0	0	3	-23.09	-21.98	328.9	-236.61	-233.9	624.88	-8.47	-7.87	551.97	0	-2.52	-0.5
2	1	17.15	0	3	219.2	66.86	9.33	349.02	-23.79	-164.58	0	-7.97	383.55	0	0	0
3	1	17.15	68.58	3	17.92	-3.73	0.07	34.81	-18.18	-8.87	0	0	194.54	0	0	0
4	1	0	68.58	3	16.25	-3.12	0.07	31.41	-16.03	-8.2	-5.77	0	189.92	0	-0.22	0
5	1	0	0	32.99	2.88	-1.61	38.41	-120.92	-194.23	459.09	19.06	2.02	290.65	-0.37	-6.36	0.07
6	4	17.15	0	32.99	5.02	-1.83	39.21	-97.48	-209.43	460.7	0	2.12	304.12	-0.38	0	0
7	4	17.15	68.58	32.99	0.94	8.06	3.83	-38.93	77.27	8.2	0	0	197.4	0	0	0
8	4	0	68.58	32.99	1.16	7.48	3.56	-32.73	70.51	6.48	6.32	0	192.76	0	-1.09	0

WESLEA for Windows - Simulation Output

Axle Type: Tandem

Tire Pressure: 550 kPa

Date: Mon Jul 14 03:08:36

2008

STRUCTURAL INFORMATION

Layer	Modulus (MPa)	Poisson	Height (cm)	Slip
1	551.6	0.35	3	1
2	137.9	0.35	13	1
3	137.9	0.35	16.99	1
4	82.7	0.35	2537	1
5	82.7	0.35	Infinite	

LOADING CONFIGURATION

Tire#	X (cm)	Y (cm)	Load (kN)	Pressure (kPa)
1	0	0	10	550
2	34.29	0	10	550
3	34.29	137.16	10	550
4	0	137.16	10	550

***PREDICTED PAVEMENT

	550 kPa	
	FATIGUE	RUTTING
Applied	100000	100000
Allowed	60338	445307
Damage	1.66	0.22

ENGINEERING RESPONSES

Loc#	Layer	Coordinates (cm)			Normal Stress (kPa)			Normal MicroStrain			Displacement (micrometer)			Shear Stress (kPa)		
		X	Y	Z	X	Y	Z	X	Y	Z	X	Y	Z	YZ	XZ	XY
1	1	0	0	3	-180	-178.5	489.2	-523.52	-519.84	1114.4	-8.55	-7.87	620.96	0	-2.49	-0.51
2	1	17.15	0	3	202	64.87	4.3	322.36	-13.32	-161.55	0	-7.97	378.63	0	0	0
3	1	17.15	68.58	3	17.88	-3.88	0.07	34.83	-18.44	-8.75	0	0	194.42	0	0	0
4	1	0	68.58	3	16.21	-3.27	0.07	31.42	-16.26	-8.09	-5.77	0	189.8	0	-0.22	0
5	1	0	0	32.99	2.71	-1.9	39.39	-125.89	-201.2	472.9	19.22	2.01	292.44	-0.37	-6.4	0.07
6	4	17.15	0	32.99	5.27	-2.11	39.58	-94.8	-215.38	465.22	0	2.11	305.49	-0.38	0	0
7	4	17.15	68.58	32.99	0.93	8.06	3.8	-38.91	77.45	7.87	0	0	197.28	0	0	0
8	4	0	68.58	32.99	1.15	7.48	3.53	-32.72	70.67	6.18	6.31	0	192.64	0	-1.09	0

WESLEA for Windows - Simulation Output

Axle Type: Single

Tire Pressure: 345 kPa

Date: Mon Jul 14 01:09:12
2008

STRUCTURAL INFORMATION

Layer	Modulus	Poisson	Height	Slip
	(MPa)		(cm)	
1	551.6	0.35	3	1
2	137.9	0.35	13	1
3	82.7	0.35	16.99	1
4	82.7	0.35	2537	1
5	82.7	0.35	Infinite	

LOADING CONFIGURATION

Tire#	X	Y	Load	Pressure
	(cm)	(cm)	(kN)	(kPa)
1	0	0	20	345
2	34.29	0	20	345

***PREDICTED PAVEMENT

	345 kPa	
	FATIGUE	RUTTING
Applied	100000	100000
Allowed	3E+07	30889
Damage	0	3.24

ENGINEERING RESPONSES

Loc#	Layer	Coordinates (cm)			Normal Stress (kPa)			Normal MicroStrain			Displacement (micrometer)			Shear Stress (kPa)		
		X	Y	Z	X	Y	Z	X	Y	Z	X	Y	Z	YZ	XZ	XY
1	1	0	0	3	130.3	142.21	339.2	-69.24	-40.06	441.95	-14.38	0	916.06	0	-6.05	0
2	1	17.15	0	3	469.6	146.09	68.87	714.96	-76.83	-265.81	0	0	798.55	0	0	0
3	1	0	0	32.99	7.35	-2.44	75.3	-219.43	-379.37	889.75	37.79	0	489.46	0	-13.09	0
4	1	17.15	0	32.99	9.68	-2.83	80.33	-210.89	-415.26	942.34	0	0	519.78	0	0	0

WESLEA for Windows - Simulation Output

Axle Type: Single

Tire Pressure: 410 kPa

Date: Mon Jul 14 01:08:27
2008

STRUCTURAL INFORMATION

Layer	Modulus (MPa)	Poisson	Height (cm)	Slip
1	551.6	0.35	3	1
2	137.9	0.35	13	1
3	82.7	0.35	16.99	1
4	82.7	0.35	2537	1
5	82.7	0.35	Infinite	

LOADING CONFIGURATION

Tire#	X (cm)	Y (cm)	Load (kN)	Pressure (kPa)
1	0	0	20	410
2	34.29	0	20	410

***PREDICTED PAVEMENT

	410 kPa	
	FATIGUE	RUTTING
Applied	100000	100000
Allowed	4E+06	29746
Damage	0.02	3.36

ENGINEERING RESPONSES

Loc#	Layer	Coordinates (cm)			Normal Stress (kPa)			Normal MicroStrain			Displacement (micrometer)			Shear Stress (kPa)		
		X	Y	Z	X	Y	Z	X	Y	Z	X	Y	Z	YZ	XZ	XY
1	1	0	0	3	107.6	120.43	401.3	-135.92	-104.56	582.74	-14.54	0	960.86	0	-5.92	0
2	1	17.15	0	3	472.4	148.05	48.35	731.8	-62.03	-306.03	0	0	789.73	0	0	0
3	1	0	0	32.99	7.17	-2.83	76.71	-225.93	-389.32	909.22	38.09	0	492.34	0	-13.17	0
4	1	17.15	0	32.99	10	-3.24	81.06	-208.42	-424.58	951.57	0	0	522.28	0	0	0

WESLEA for Windows - Simulation Output

Axle Type: Single
Tire Pressure: 550 kPa

Date: Mon Jul 14 01:07:32
2008

STRUCTURAL INFORMATION

Layer	Modulus (MPa)	Poisson	Height (cm)	Slip
1	551.6	0.35	3	1
2	137.9	0.35	13	1
3	82.7	0.35	16.99	1
4	82.7	0.35	2537	1
5	82.7	0.35	Infinite	

LOADING CONFIGURATION

Tire#	X (cm)	Y (cm)	Load (kN)	Pressure (kPa)
1	0	0	20	550
2	34.29	0	20	550

***PREDICTED PAVEMENT

	550 kPa	
	FATIGUE	RUTTING
Applied	100000	100000
Allowed	348064	28322
Damage	0.29	3.53

ENGINEERING RESPONSES

Loc#	Layer	Coordinates (cm)			Normal Stress (kPa)			Normal MicroStrain			Displacement (micrometer)			Shear Stress (kPa)		
		X	Y	Z	X	Y	Z	X	Y	Z	X	Y	Z	YZ	XZ	XY
1	1	0	0	3	38.43	52.33	530.3	-300.03	-266	903.82	-14.75	0	1041.4	0	-5.73	0
2	1	17.15	0	3	453.3	146.87	27.66	711.03	-38.92	-330.66	0	0	778.39	0	0	0
3	1	0	0	32.99	6.89	-3.4	78.73	-235.48	-403.56	937.28	38.51	0	496.37	0	-13.28	0
4	1	17.15	0	32.99	10.48	-3.8	82.03	-204.35	-437.58	963.7	0	0	525.67	0	0	0

WESLEA for Windows - Simulation Output

Axle Type: Single

Tire Pressure: 690 kPa

Date: Mon Jul 14 01:06:10
2008

STRUCTURAL INFORMATION

Layer	Modulus (MPa)	Poisson	Height (cm)	Slip
1	551.6	0.35	3	1
2	137.9	0.35	13	1
3	82.7	0.35	16.99	1
4	82.7	0.35	2537	1
5	82.7	0.35	Infinite	

LOADING CONFIGURATION

Tire#	X (cm)	Y (cm)	Load (kN)	Pressure (kPa)
1	0	0	20	690
2	34.29	0	20	690

***PREDICTED PAVEMENT

	690 kPa	
	FATIGUE	RUTTING
Applied	100000	100000
Allowed	78107	27538
Damage	1.28	3.63

ENGINEERING RESPONSES

Loc#	Layer	Coordinates (cm)			Normal Stress (kPa)			Normal MicroStrain			Displacement (micrometer)			Shear Stress (kPa)		
		X	Y	Z	X	Y	Z	X	Y	Z	X	Y	Z	YZ	XZ	XY
1	1	0	0	3	-50.1	-35.57	652.5	-482.3	-446.73	1237.3	-14.86	0	1106.9	0	-5.61	0
2	1	17.15	0	3	434.1	145.05	18.57	683.21	-24.29	-333.83	0	0	772.05	0	0	0
3	1	0	0	32.99	6.7	-3.76	80	-241.62	-412.51	955	38.75	0	498.84	0	-13.34	0
4	1	17.15	0	32.99	10.79	-4.16	82.6	-201.5	-445.55	970.72	0	0	527.7	0	0	0

WESLEA for Windows - Simulation Output

Axle Type: Tridem

Tire Pressure: 410 kPa

Date: Mon Jul 14 01:26:44
2008

STRUCTURAL INFORMATION

Layer	Modulus (MPa)	Poisson	Height (cm)	Slip
1	551.6	0.35	3	1
2	137.9	0.35	13	1
3	137.9	0.35	16.99	1
4	82.7	0.35	2537	1
5	82.7	0.35	Infinite	

LOADING CONFIGURATION

Tire#	X (cm)	Y (cm)	Load (kN)	Pressure (kPa)
1	0	0	7	550
2	34.29	0	7	550
3	34.29	137.16	7	550
4	0	137.16	7	550
5	0	274.32	7	550
6	34.29	274.32	7	550

***PREDICTED PAVEMENT

	410 kPa	
	FATIGUE	RUTTING
Applied	100000	100000
Allowed	139810	2E+06
Damage	0.72	0.06

ENGINEERING RESPONSES

Loc#	Layer	Coordinates (cm)			Normal Stress (kPa)			Normal MicroStrain			Displacement (micrometer)			Shear Stress (kPa)		
		X	Y	Z	X	Y	Z	X	Y	Z	X	Y	Z	YZ	XZ	XY
1	1	0	0	3	-146.1	-145.8	360.2	-400.87	-400.26	838.27	-6.18	-8.58	458.5	0	-1.74	-0.4
2	1	17.15	0	3	140.6	44.91	2.72	224.65	-9.52	-112.76	0	-8.66	281.87	0	0	0
3	1	17.15	68.58	3	13.34	-3.35	0.05	26.27	-14.57	-6.25	0	-3.92	158.93	0	0	0
4	1	0	68.58	3	12.16	-2.89	0.05	23.85	-13	-5.79	-4.36	-3.9	155.62	0	-0.15	-0.11
5	1	17.15	137.2	3	141.8	43.89	2.72	227.49	-12.13	-112.88	0	0	299.03	0	0	0
6	4	0	0	32.99	1.94	-1.3	27.65	-88.04	-141.01	331.65	13.39	0.16	222.04	-0.28	-4.48	0.05
7	4	17.15	0	32.99	3.77	-1.44	27.74	-65.69	-150.85	325.57	0	0.22	231.18	-0.29	0	0
8	4	17.15	68.58	32.99	0.74	5.8	2.67	-26.88	55.67	4.58	0	-0.7	161.1	-0.06	0	0
9	4	0	68.58	32.99	0.89	5.39	2.48	-22.54	50.9	3.41	4.36	-0.71	157.78	-0.06	-0.77	0.01
10	4	17.15	137.2	32.99	3.86	-0.92	27.8	-67.11	-145.18	323.78	0	0	248.7	0	0	0